

**Rigid Frame Porous Materials: Fundamental Theory and
Applications**

S. Rossetti, P. Gardonio and M.J. Brennan

ISVR Technical Memorandum 911

May 2003



SCIENTIFIC PUBLICATIONS BY THE ISVR

Technical Reports are published to promote timely dissemination of research results by ISVR personnel. This medium permits more detailed presentation than is usually acceptable for scientific journals. Responsibility for both the content and any opinions expressed rests entirely with the author(s).

Technical Memoranda are produced to enable the early or preliminary release of information by ISVR personnel where such release is deemed to be appropriate. Information contained in these memoranda may be incomplete, or form part of a continuing programme; this should be borne in mind when using or quoting from these documents.

Contract Reports are produced to record the results of scientific work carried out for sponsors, under contract. The ISVR treats these reports as confidential to sponsors and does not make them available for general circulation. Individual sponsors may, however, authorize subsequent release of the material.

COPYRIGHT NOTICE

(c) ISVR University of Southampton All rights reserved.

ISVR authorises you to view and download the Materials at this Web site ("Site") only for your personal, non-commercial use. This authorization is not a transfer of title in the Materials and copies of the Materials and is subject to the following restrictions: 1) you must retain, on all copies of the Materials downloaded, all copyright and other proprietary notices contained in the Materials; 2) you may not modify the Materials in any way or reproduce or publicly display, perform, or distribute or otherwise use them for any public or commercial purpose; and 3) you must not transfer the Materials to any other person unless you give them notice of, and they agree to accept, the obligations arising under these terms and conditions of use. You agree to abide by all additional restrictions displayed on the Site as it may be updated from time to time. This Site, including all Materials, is protected by worldwide copyright laws and treaty provisions. You agree to comply with all copyright laws worldwide in your use of this Site and to prevent any unauthorised copying of the Materials.

UNIVERSITY OF SOUTHAMPTON
INSTITUTE OF SOUND AND VIBRATION RESEARCH
DYNAMICS GROUP

**Rigid Frame Porous Materials:
Fundamental Theory and Applications**

by

S. Rossetti, P. Gardonio and M.J. Brennan

ISVR Technical Memorandum No: 911

May 2003

Authorised for issue by
Professor M.J. Brennan
Group Chairman

ACKNOWLEDGEMENTS

The work carried out by Silvia Rossetti has been supported by the European Community through a Marie Curie Fellowship within the EDSVS – European Doctorate in Sound and Vibration Studies.

Ms Rossetti would like to thank her Home Supervisor prof. Roberto Zecchin for his constant support and encouragement during the fellowship and the whole Ph.D.

INDEX

1	INTRODUCTION	1
2	WAVE PROPAGATION IN AIR AND IN POROUS MEDIA	3
2.1	ACOUSTIC WAVE IN AIR	3
2.2	WAVES IN A POROUS MATERIAL.....	4
2.3	SUMMARY	6
3	REFLECTION AND TRANSMISSION OF WAVES FROM ONE MEDIUM TO ANOTHER	7
3.1	INTRODUCTION	7
3.2	WAVES IMPINGING A SEMI INFINITE POROUS MATERIAL	7
3.2.1	<i>Definitions</i>	<i>7</i>
3.2.2	<i>Representation of waves in the spatial domain</i>	<i>9</i>
3.3	WAVES IMPINGING A FINITE THICKNESS MEDIUM	10
3.3.1	<i>Positive going waves inside the layer.....</i>	<i>12</i>
3.3.2	<i>Negative going waves inside the layer</i>	<i>14</i>
3.3.3	<i>Considerations on the reflection coefficient.....</i>	<i>15</i>
3.3.4	<i>Representation of waves in a rigidly backed layer of porous material.....</i>	<i>18</i>
3.4	ACOUSTIC ABSORPTION	20
3.5	ABSORPTION AND TRANSMISSION OF A LAYER OF POROUS MATERIAL WITHOUT RIGID BACKING	23
3.6	ABSORPTION OF A POROUS LAYER AT A CERTAIN DISTANCE FROM A RIGID WALL ..	27
3.6.1	<i>Waves in the air gap between the porous material and the rigid backing ..</i>	<i>27</i>
3.6.2	<i>Plateau height.....</i>	<i>33</i>
3.6.3	<i>Peaks of absorption</i>	<i>35</i>
3.7	POROSITY	38
4	CONCLUDING REMARKS	40
	APPENDIX A.....	41
	APPENDIX B.....	46
	APPENDIX C.....	50
	REFERENCES	52

NOMENCLATURE

α	attenuation constant
α_{∞}	tortuosity
β	propagation constant
ϕ	angle
γ	ratio of the specific heats
η	dynamic viscosity
κ	bulk modulus
λ_i	wavelength of sound at the tuned frequency ω_i
θ	angle
ρ_0	equilibrium density at (x,y,z)
ρ	instantaneous density at (x,y,z)
σ	flow resistivity
ω	circular frequency
Ω	normalised frequency
c	phase speed of sound
d	thickness of the layer
f	force
g	gravitational force
h	porosity
k	wavenumber
m	mass
p	acoustic pressure at the generic position (x,y,z)
q	condensation
r, r_{ij}	surface reflection coefficient
s	structure factor
t	time
t_{ij}	surface transmission coefficient
u	particle velocity
u'	volume velocity of flow per unit cross sectional area
z	characteristic impedance
A	absorption coefficient
B	adiabatic modulus
D	layer thickness plus cavity depth
P_i	complex amplitude of the sound wave
P_0	equilibrium pressure at (x,y,z)
P	instantaneous pressure at (x,y,z)
R	reflection coefficient
V	volume

ABSTRACT

Several researchers have investigated the acoustic properties of rigid frame porous materials. Models for these materials require the definition of several parameters, which generally need to be measured through different procedures. The work presented in this report concerns the behaviour of porous media when exposed to a normal incidence sound field. A short section on the fundamental theory of wave propagation in air and in a porous material is first presented. Then the approach based on simple concepts of wave propagation in semi-infinite materials and in rigidly backed porous layers is described. Relatively simple expressions for reflection and acoustic absorption coefficients are derived and compared with established equations. The derivation is extended also to the case of a layer of porous medium placed at a certain distance from a rigid wall. Some practical considerations about common installation of layers of porous absorbing materials are finally presented.

1 INTRODUCTION

The use of sound absorbing materials is widespread, for example in noise control and acoustic design of auditoria and rooms. Absorption mechanisms are divided into three main groups, according to the way in which acoustic energy is dissipated:

- porous materials;
- panel absorbers;
- cavity resonators.

Porous materials, such as acoustic tiles and plasters, mineral wools (fibreglass), carpets, and draperies consist of networks of interconnected pores within which viscous losses convert acoustic energy into heat. The absorption effects of such materials strongly depend on frequency: they are relatively small at low frequency and they increase to relatively high values with frequency. They also increase with increasing thickness of the lining. Mounting the material away from the wall can increase low frequency absorption (Richardson, 1953).

A *panel absorber* mounted away from a solid backing vibrates under the influence of the incident sound, and the dissipative mechanisms in the panel convert some of the incident acoustic energy into heat. Such absorbers (gypsum sheetrock, plywood, thin wooden panelling, etc) are quite effective at low frequency absorption (Richardson, 1953).

A *cavity resonator* consists of a confined volume of air connected to the acoustic field to be controlled by a narrow opening or a small neck. It acts like a Helmholtz resonator, which absorbs acoustic energy most efficiently in a narrow band of frequencies near its resonance frequency. This type of acoustic treatment may be in the form of individual elements, such as concrete blocks with slotted cavities. Other forms consist of perforated panels and wood lattices spaced away from a solid backing with absorption blankets in between. They provide useful absorption over a wider frequency range than is possible with individual cavity elements (Kuttruff, 1973).

The research presented in this report focuses on the behaviour of the first type of absorbing materials, i.e. porous materials. In order to understand their acoustic behaviour it is necessary to investigate in detail their physical properties. This area has been extensively investigated from a non-acoustical point of view, i.e. in the field of dynamics of fluids (Johnson *et al*, 1987 and Lafarge *et al*, 1997). Many researchers have tried to describe the physics of these systems by modelling the behaviour of fluids inside the pores of the material from a macro or microscopic point of view (Umnova *et al*, 2000). The theory in this field is quite complex and simplification is necessary in order to connect it with the practical applications of this kind of material. Work in this sense has been described by Brennan and To (2001), and the purpose of the study presented in this report is to present a complete and consistent analysis of rigid frame porous materials from a macroscopic point of view, with a set of simple formulae and graphs to help engineers design and implement acoustic treatments of this type.

Following this introduction, in section 2 the wave equation in air and then in porous media is presented together with the relative harmonic solutions. Section 3 offers a detailed insight into the absorption properties of porous materials. It starts with the general definitions and representations of waves impinging a semi-infinite medium, characterised by ideal zero dissipation, and then describes the case of a semi-infinite porous medium. The same approach is used for a finite thickness layer with a rigid backing, where standing waves are generated between a surface of the layer and the rigid wall. An interesting

extension of this work has also been studied, that is the case of sound transmission through a finite thickness layer of porous material. Finally the case of a porous layer placed at a fixed distance from a rigid wall has also been analysed, which represents a common application in architectural acoustics.

Through the whole of this report only plane incident waves are considered and while analysing waves impinging semi infinite and finite thickness layers of porous media the assumption of local reaction is made. The 'normal surface specific acoustic impedance' depends on the form of the incident wave. In fact the normal component of the particle velocity at any one point on the interface is influenced not only by the local sound pressure, but also by waves arriving from all other points of the exciting medium. Consequently in general it is not possible to specify unique boundary impedance, independent of the amplitude and phase distributions of the incident wave over the interface. As porous sound-absorbing materials are selected for their capacity to dissipate sound energy efficiently, and therefore to attenuate propagating waves, acoustic communication within such material is rather ineffective. Consequently in many cases it is reasonable to assume that the particle velocity generated by incident sound at any point on the surface of a material is linearly related only to the local sound pressure, and is therefore independent of the form of the incident sound field. The material is said to exhibit 'local reaction' and it can be characterised by unique surface boundary impedance. The condition of zero tangential velocity is not applicable to an interface between two fluid media or to that between a fluid medium and a fluid saturated solid. However this component of particle velocity is not relevant to the transfer of sound energy across an interface, which is a function of only the normal component (Fahy, 2001).

2 WAVE PROPAGATION IN AIR AND IN POROUS MEDIA

This section gives the basic definitions and equations of acoustic waves, first in air and then in a rigid frame porous material. The aim is to describe the physical behaviour of waves and analyse the parameters that characterise porous materials from an acoustical point of view. The concepts of complex impedance, wavenumber and density are introduced, which are applied in section 3 to the general case of a semi-infinite porous material and then to the case of a finite thickness layer of porous material.

2.1 Acoustic wave in air

The *linear, lossless wave equation* for the propagation of sound in fluids with phase speed c is (see appendix A and Kinsler *et al*, 2000):

$$\nabla^2 p = \frac{1}{c^2} \frac{\partial^2 p}{\partial t^2} \quad (2.1)$$

where p is the acoustic pressure at (x,y,z)

t is the time

and $\nabla^2 = \frac{\partial}{\partial x^2} + \frac{\partial}{\partial y^2} + \frac{\partial}{\partial z^2}$ is the Laplacian operator in x, y, z directions of a right

handed Cartesian coordinate system of reference.

The particular case of *harmonic motion* is considered with reference to a plane wave, which propagates in an isotropic medium. For homogeneous isotropic fluids the speed of sound is a constant throughout the medium. Also each acoustic variable of a plane wave has constant amplitude and phase on any plane perpendicular to the direction of propagation. Assuming the plane wave propagates along the x -axis, the wave equation becomes:

$$\frac{\partial^2 p}{\partial x^2} = \frac{1}{c^2} \frac{\partial^2 p}{\partial t^2} \quad (2.2)$$

and, assuming harmonic wave propagation, the general solution can be expressed in the following complex form

$$p(x,t) = Ae^{j(\omega t - kx)} + Be^{j(\omega t + kx)} \quad (2.3)$$

where A and B are two arbitrary constants, ω is the circular frequency and k is the acoustic wavenumber ($k = \omega / c$). The actual sound pressure will be taken to be the real part of $p(x,t)$, even though this will be omitted throughout this report.

The associated particle velocity $u(x,t)$ is, in this case, parallel to the direction of propagation and therefore given by (Kinsler *et al*, 2000)

$$u(x,t) = (A/\rho_0 c)e^{j(\omega t - kx)} - (B/\rho_0 c)e^{j(\omega t + kx)} \quad (2.4)$$

where ρ_0 is the density of the fluid.

The sound pressure given by equation (2.3) can also be divided into two components

$$p_+ = Ae^{j(\omega t - kx)} \quad \text{and} \quad p_- = Be^{j(\omega t + kx)}, \quad (2.5)$$

which physically represent the sound pressure of positive and negative going waves respectively, with reference to $x = 0$.

2.2 Waves in a porous material

The derivation of the wave equation is now extended to the case of propagation of sound in a porous medium. The particular case of a plane wave propagating in x -direction is considered. The modified wave equation for plane wave sound propagation in gases contained within rigid porous materials can be derived from the equation of *mass conservation* and the *momentum equation*, as described in detail in Chapter 7 of reference (Fahy, 2001). The conservation of mass results in the following equation

$$\left(\frac{\rho_0}{\kappa} \right) \frac{\partial p}{\partial t} + \left(\frac{\rho_0}{h} \right) \frac{\partial u'}{\partial x} = 0 \quad (2.6)$$

where κ is the effective bulk modulus of the gas, h the porosity of the material and u' is the cross-sectional average particle velocity. The bulk modulus refers to the ratio of pressure to the decrease in volume and its inverse is the compressibility. Applying the principle of conservation of momentum gives

$$\frac{\partial p}{\partial x} = - \left(\frac{s\rho_0}{h} \right) \frac{\partial u'}{\partial t} - \sigma u' \quad (2.7)$$

where σ is the flow resistivity and s is the structure factor. The presence of the porosity in the first term of the right hand side of eq. (2.7) indicates that the average particle acceleration within the pores of the material is greater by a factor h than the volume acceleration per unit area which is represented by $\frac{\partial u'}{\partial t}$. In the case of harmonic motion with circular frequency ω , then equation (2.7) becomes

$$\frac{\partial p}{\partial x} = - \left(\frac{s\rho_0}{h} - j \frac{\sigma}{\omega} \right) \frac{\partial u'}{\partial t} \quad (2.8)$$

and the term

$$\rho' = \left(\frac{s\rho_0}{h} - j \frac{\sigma}{\omega} \right) \quad (2.9)$$

can be considered as a complex density. Equation (2.8) shows that the harmonic pressure and particle acceleration in a plane wave are not in quadrature inside a porous medium as they are in free space. The ratio of the real to the imaginary part of the complex density increases with frequency. This means that viscosity controls low frequency propagation and inertia controls high-frequency propagation.

The modified plane wave equation

Differentiation of eq. (2.6) with respect to time and of eq. (2.7) with respect to x , and elimination of the common term, produces the following modified plane wave equation:

$$\frac{\partial^2 p}{\partial x^2} - \left(\frac{s\rho_0}{\kappa} \right) \frac{\partial^2 p}{\partial t^2} - \left(\frac{\sigma h}{\kappa} \right) \frac{\partial p}{\partial t} = 0 \quad (2.10)$$

The main effects of parameters h , s and σ , together with altered bulk modulus κ , are:

- 1) to alter the speed of propagation of plane waves from its free wave value and
- 2) to attenuate the wave as it propagates.

Harmonic solution of the modified plane wave equation

The harmonic solution of the modified plane wave equation can then be written in complex form as

$$p(x,t) = Ae^{(-jk'x)}e^{(j\omega t)} \quad \text{or} \quad p(x,t) = Ae^{j(\omega t - k'x)} \quad (2.11)$$

where A is the complex amplitude. The complex wavenumber k' takes the place of k in the free wave equation (2.10), and it can be written in the following form:

$$k' = \beta - j\alpha, \quad (2.12)$$

in which α is the *attenuation constant* and β is the *propagation constant*. The imaginary component of the wavenumber k' represents the real part of the exponent, and is referred to as attenuation constant as it is responsible for the attenuation of sound. The real phase speed of a plane wave propagating in a porous medium is given by ω / β . Substitution into equation (2.10) of eq. (2.11) yields

$$(-k'^2 + \frac{\omega^2 s\rho_0}{\kappa} - \frac{j\omega\sigma h}{\kappa})p = 0 \quad (2.13)$$

or

$$k'^2 = \omega^2 \left(\frac{s\rho_0}{\kappa} - \frac{j\sigma h}{\omega\kappa} \right) \quad (2.14)$$

which can be written as

$$k'^2 = \left(\frac{\omega^2 h}{\kappa}\right) \rho' \quad (2.15)$$

Substitution of this expression into eq. (2.8) gives an equation for the characteristic specific acoustic impedance of a porous medium:

$$z_c = \frac{p(x)}{u'(x)} = \frac{\rho' \omega}{k'} = \left(\frac{\rho' k'}{h}\right)^{\frac{1}{2}} = \frac{\kappa k'}{\omega h} \quad (2.16)$$

which is complex, indicating that the particle velocity is not in phase with the pressure.

2.3 Summary

In this section the fundamental definitions and equations of acoustic waves have been given. Distinction between the cases of waves in air and in porous materials have been presented, with considerations about the influences on the main acoustic parameters: density, speed of sound, wavenumber and impedance. The basic definitions and equations presented here are necessary foundations for the work presented in the following section.

3 REFLECTION AND TRANSMISSION OF WAVES FROM ONE MEDIUM TO ANOTHER

3.1 Introduction

The fundamental equations governing the behaviour of a plane wave propagating in the x -direction, given in the previous section, are now applied to the cases where a propagating wave in a medium impinges another medium of semi infinite and finite thickness. In both cases calculations for the simple case of a medium with real density, specific impedance, wavenumber and speed of sound are first presented. Next the case of a porous medium is considered in which case these parameters are complex.

The *reflection* and *transmission* coefficients at the interface between the two media are first introduced and equations for the standing waves inside the layer are then derived. Reflection coefficients are also derived for the case of transmission through a finite thickness medium placed at a certain distance from a rigid wall, as they are necessary for the computation of absorption coefficients. Some of the results obtained are then compared with established equations in order to verify the reliability of the model. Within the model specific parameters concerning the physical and acoustical properties of a porous material have been used and they are given in Appendix C.

3.2 Waves impinging a semi infinite porous material

3.2.1 Definitions

A simple representation of a propagating time harmonic wave in a generic medium 1 which impinges on a semi-infinite medium 2 is shown in Figure 3.1 where ρ_1 and c_1 are the density and speed of sound in the fluid on the left hand side respectively and ρ_2 and c_2 are the density and speed of sound in the fluid or porous material on the right hand side respectively.

The wave impinging on medium 2 (incident wave) is partly absorbed/dissipated inside the medium itself, and partly reflected.

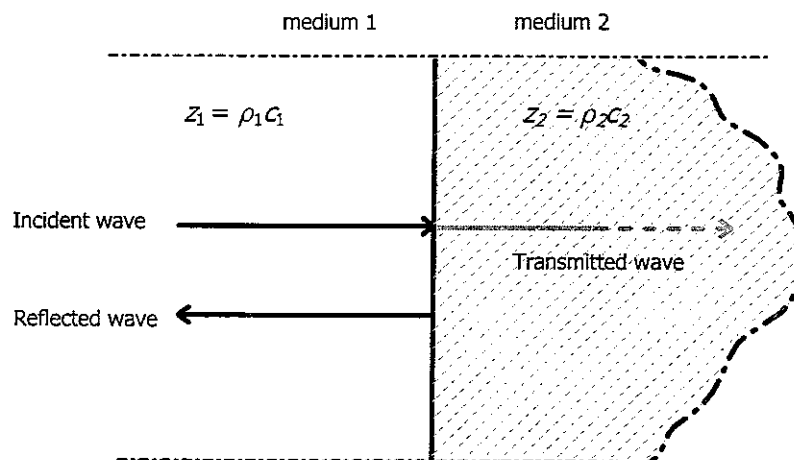


Figure 3.1 Representation of waves in a semi-infinite medium

For this system the *reflection* and *transmission* coefficients can be specified, as follows. The *interface reflection coefficient* is defined as the ratio between the reflected and the incident sound pressure

$$r = \frac{p_r}{p_i} = \frac{P_r}{P_i} \quad (3.1)$$

whereas the *interface transmission coefficient* is equal to the ratio

$$t = \frac{p_t}{p_i} = \frac{P_t}{P_i} \quad (3.2)$$

where

$$p_i = P_i e^{j(\omega x - k_1 x)} \quad (3.3)$$

$$p_r = P_r e^{j(\omega x + k_1 x)} \quad (3.4)$$

$$p_t = P_t e^{j(\omega x - k_2 x)} \quad (3.5)$$

are the expressions for the sound pressure of the incident, reflected and transmitted waves and P_i , P_r and P_t are the relative complex amplitudes (phasors) for $t = 0$ and $x = 0$ at the interface.

By taking into account the continuity of pressure and of the normal component of the particle velocity at the interface between the two media (see Kinsler *et al*, 2000 for more details), it is possible to derive expressions for both r and t

$$r = \frac{z_2 - z_1}{z_2 + z_1} \quad (3.6)$$

$$t = \frac{2z_2}{z_2 + z_1} \quad (3.7)$$

where $z_1 = \rho_1 c_1$ and $z_2 = \rho_2 c_2$ are the characteristic impedances of the two media.

Now a distinction has to be made between two cases: first waves impinging a fluid of different characteristics and second, waves impinging on a porous medium, characterised by its complex density, impedance and wavenumber.

In the first case, the interface reflection coefficient r is always real. It is positive when $z_2 > z_1$ and negative when $z_2 < z_1$. Consequently at the boundary the acoustic pressure of the reflected wave is either in phase or 180° out of phase with that of the incident wave. When the characteristic acoustic impedance of fluid 2 is greater than that of fluid 1, a

positive pressure of the incident wave is reflected as a positive pressure. On the other hand, if $z_2 < z_1$, the positive pressure of the incident wave is reflected as a negative pressure. The interface transmission coefficient t is real and positive regardless of the relative magnitudes of z_2 and z_1 . Consequently at the boundary the acoustic pressure of the transmitted wave is always in phase with that of the incident wave. In the second case the incident and reflected pressures are not always exactly in phase, and thus the normal specific acoustic impedance may be a complex quantity

$$z = z_r + jz_i, \quad (3.8)$$

where z_r is the resistance and z_i the reactance. The general surface reflection coefficient becomes

$$r = \frac{(z_r - z_1) + jz_i}{(z_r + z_1) + jz_i}. \quad (3.9)$$

Furthermore, inside the layer there is dissipation, and thus the density and speed of sound are complex quantities.

3.2.2 Representation of waves in the spatial domain

The harmonic time dependence is now suppressed for clarity, so that the expressions for the incident, reflected and transmitted waves become:

$$p_i = P_i e^{-jk_1 x} \quad (3.10)$$

$$p_r = P_r e^{+jk_1 x} = r P_i e^{+jk_1 x} \quad (3.11)$$

$$p_t = P_t e^{+jk_2 x} = t P_i e^{+jk_2 x}. \quad (3.12)$$

They are plotted in Figure 3.2 for the general case of separation between two fluids, so that both the impedances z_1 and z_2 are real, and in Figure 3.3 for waves impinging a porous material, so that ρ_2 , k_2 , z_2 and c_2 are complex.

By comparing the two figures, the additional effects generated by the porous medium, of amplitude decay through the medium itself and phase shift of the reflected wave, are clearly seen.

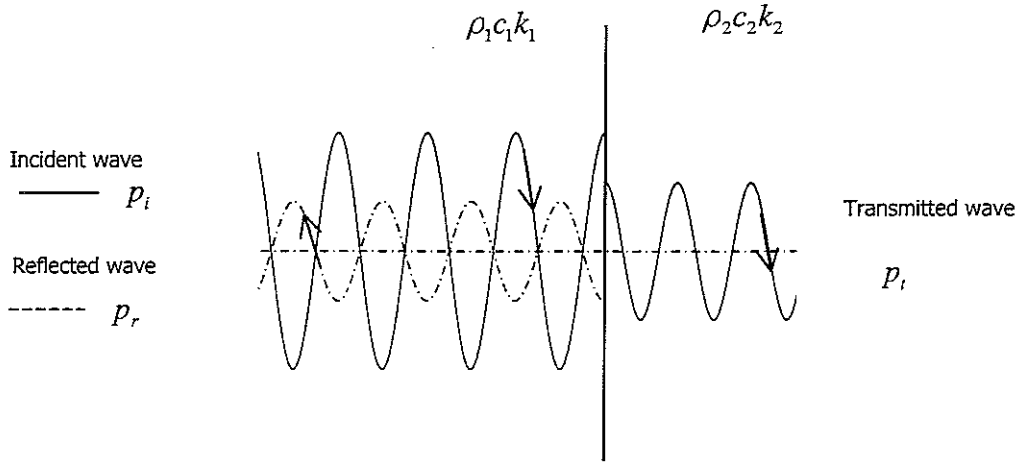


Figure 3.2 *Incident, transmitted and reflected waves in a simple case of separation between two fluids (air/vapour)*

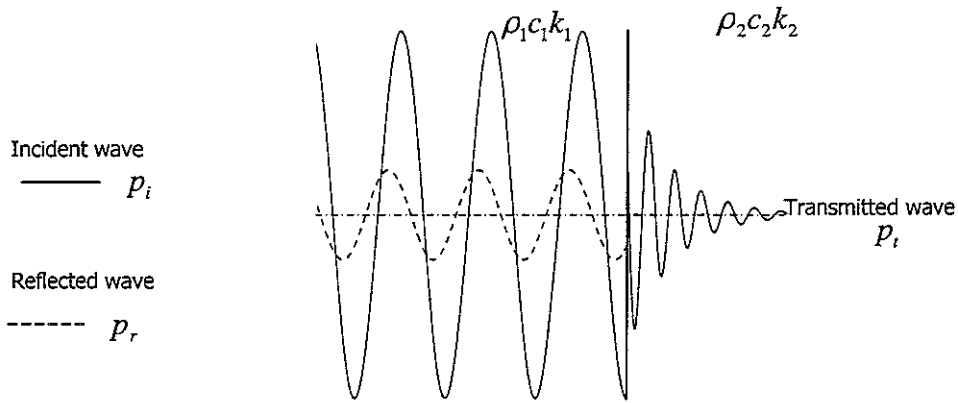


Figure 3.3 *Incident, transmitted and reflected waves in a simple case of waves impinging a semi infinite porous material*

3.3 Waves impinging a finite thickness medium

For a semi-infinite medium, waves are only reflected at the surface of the medium itself, while transmitted waves are progressively dissipated inside it. In the case of a finite thickness medium, the waves transmitted inside the layer are also reflected by the rear surface. Thus, when considering a finite thickness layer of fluid or porous medium, interface reflection and transmission coefficients for both directions have to be considered (see Figure 3.4). Considering equations (3.6) and (3.7), and the notation shown in Figure 3.4, the following interface reflection and transmission coefficients can be defined:

$$r_{12} = \frac{z_2 - z_1}{z_2 + z_1} \quad r_{21} = \frac{z_1 - z_2}{z_1 + z_2} \quad (3.13)$$

$$t_{12} = \frac{2z_2}{z_2 + z_1} \quad t_{21} = \frac{2z_1}{z_2 + z_1} \quad (3.14)$$

$$r_{23} = \frac{z_3 - z_2}{z_3 + z_2} \quad r_{32} = \frac{z_2 - z_3}{z_2 + z_3} \quad (3.15)$$

$$t_{23} = \frac{2z_3}{z_3 + z_2} \quad t_{32} = \frac{2z_2}{z_3 + z_2} \quad (3.16)$$

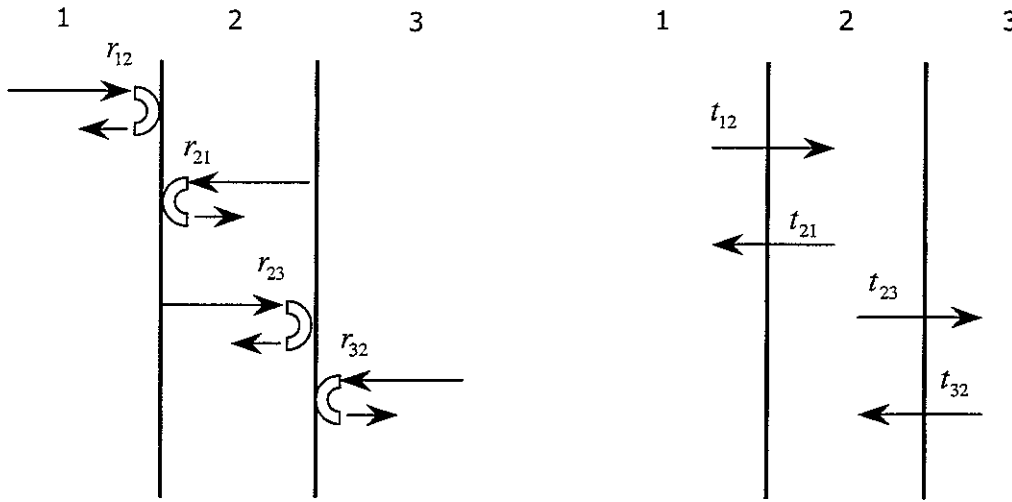


Figure 3.4 Schematisation of the interface reflection and transmission indexes at the two surfaces separating media 1 and 2 and media 2 and 3

When dealing with finite-thickness layers of materials further reflection and transmission coefficients, here indicated with capital letters, can be defined. As shown in Figure 3.5, the overall reflection coefficient R at the left hand side of the layer includes the contribution not only of the surface reflection, but also that of the waves inside the layer. The transmission coefficient T is instead representative of transmission not only through an interface (e.g. one of the two surfaces of a layer), but of the whole layer itself.

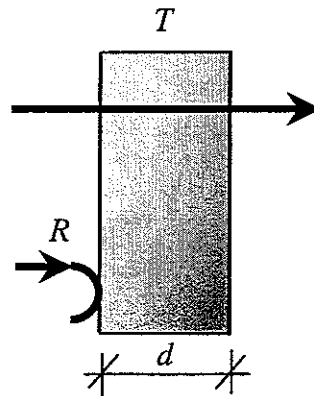


Figure 3.5 Reflection and transmission coefficients R and T

If the layer of fluid or porous medium is rigidly backed, then coefficients r_{32} and t_{32} are not defined, whereas $r_{23} = 1$ (as z_3 is assumed to be infinite) and $t_{23} = 0$.

In the following subsections the reflection coefficient R for a rigidly backed layer of fluid or porous material is first derived. In section 3.5 the reflection and transmission coefficients (R and T) of a layer without rigid backing are then calculated, and finally section 3.6 defines the overall reflection coefficient R for the case of a layer placed at a certain distance from a rigid wall. For the last case, the locally reacting model applies, as the air gap is assumed to have rigid partitions (Kuttruff, 1973).

In order to describe the behaviour of waves inside the layer, the sound pressure is expressed in terms of two components: one due to positive going waves and another one due to negative going waves, which are analytically derived in the following sections.

3.3.1 Positive going waves inside the layer

Considering the system shown in Figure 3.6, and assuming an incident wave $p_i = P_i e^{-jk_1 x}$, the sound pressure due to the positive going waves inside the layer is given by:

$$p^+(x) = P_i t_{12} e^{-jkx} + \left\{ P_i t_{12} e^{-jkx} \right\} \left\{ e^{-jk(d-x)} r_{23} e^{-jkd} r_{21} e^{-jkx} \right\} + \left\{ P_i t_{12} e^{-jkx} \right\} \left\{ e^{-jk(d-x)} r_{23} e^{-jkd} r_{21} e^{-jkx} \right\} \left\{ e^{-jk(d-x)} r_{23} e^{-jkd} r_{21} e^{-jkx} \right\} + \dots \quad (3.17)$$

which corresponds to:

$$p^+(x) = P_i t_{12} e^{-jkx} + \left\{ P_i t_{12} e^{-jkx} \right\} \left\{ r_{21} r_{23} e^{-jk2d} \right\} + \left\{ P_i t_{12} e^{-jkx} \right\} \left\{ r_{21} r_{23} e^{-jk2d} \right\} \left\{ r_{21} r_{23} e^{-jk2d} \right\} + \dots \quad (3.18)$$

where d is the thickness of the layer and k stands for k_2 (second medium). Then, writing

$$a = P_i t_{12} e^{-jk_2 x} \quad \text{and} \quad b = r_{21} r_{23} e^{-jk_2 2d}, \quad (3.19)$$

the expression for the sound pressure of the positive waves becomes

$$p^+(x) = a + ab + ab^2 + ab^3 + \dots = a(1 + b + b^2 + b^3 + \dots) = a \sum_{i=0}^n b^i. \quad (3.20)$$

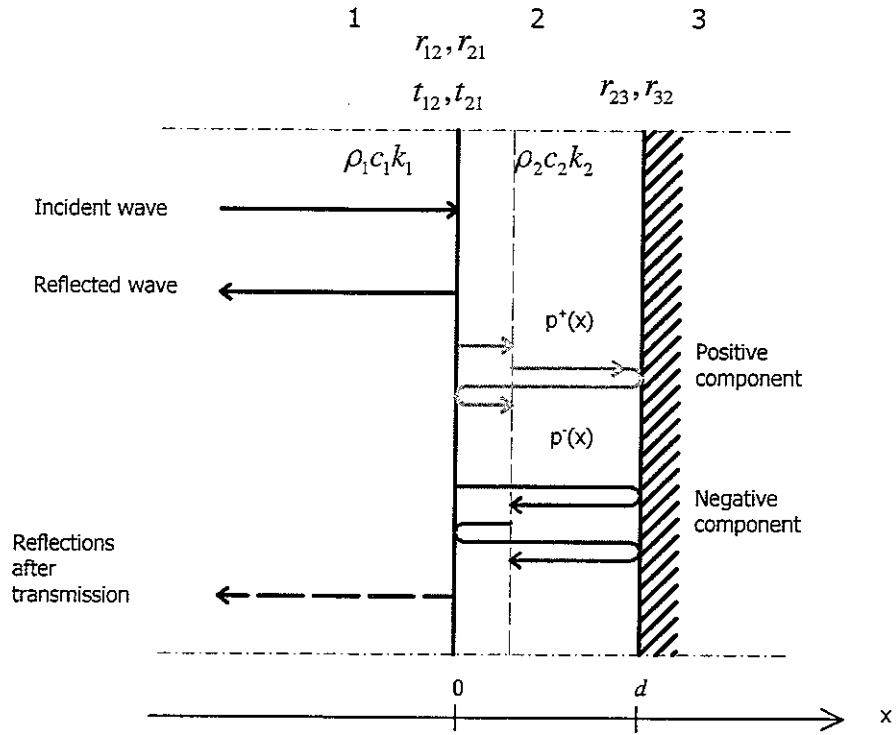


Figure 3.6 Schematic showing the reflected and transmitted waves in a finite thickness layer with rigid backing

The sum for the series in equation (3.20) is

$$p^+(x) = a \left(\frac{1}{1-b} \right) \quad (3.21)$$

that is, in terms of travelling waves,

$$p^+(x) = \frac{P_i t_{12} e^{-jk_2 x}}{1 - \{r_{21} r_{23} e^{-jk_2 2d}\}} \quad (3.22)$$

This is equivalent to writing:

$$p^+(x) = P_i t_{12} e^{-jk_2 x} + p^+(x) \{r_{21} r_{23} e^{-jk_2 2d}\} \quad (3.23)$$

The sound pressure complex amplitude of the sum of all *positive waves* inside the layer in $x=0$ is then given by:

$$p^+(0^+) = \frac{P_i t_{12}}{1 - \{r_{21} r_{23} e^{-jk_2 2d}\}} \quad (3.24)$$

In the case of rigid backing, the reflection coefficient at the right hand side interface, r_{23} , is equal to 1, and thus

$$p^+(0^+) = \frac{P_{t12}}{1 - \{r_{21} e^{-jk_2 2d}\}} \quad (3.25)$$

If there is not much dissipation inside the layer to cancel the reflection from the rear surface, then standing waves are generated inside the layer itself.

3.3.2 Negative going waves inside the layer

In the same way as in the previous subsection, the sound pressure due to the negative going waves inside the layer is given by (see Figure 3.6)

$$p^-(x) = \{P_{t12} e^{-jkd} r_{23} e^{jk(d-x)}\} + \{P_{t12} e^{-jkd} r_{23} e^{jk(x-d)}\} \{e^{+jkx} r_{21} e^{-jkd} r_{23} e^{jk(x-d)}\} + \\ + \{P_{t12} e^{-jkd} r_{23} e^{jk(x-d)}\} \{e^{+jkx} r_{21} e^{-jkd} r_{23} e^{jk(x-d)}\} \{e^{+jkx} r_{21} e^{-jkd} r_{23} e^{jk(x-d)}\} + \dots \quad (3.26)$$

which corresponds to:

$$p^-(x) = \{P_{t12} r_{23} e^{jk(x-2d)}\} + \{P_{t12} r_{23} e^{jk(x-2d)}\} \{r_{21} r_{23} e^{-jk2d}\} + \\ + \{P_{t12} r_{23} e^{-jkx}\} \{r_{21} r_{23} e^{-jk2d}\} \{r_{21} r_{23} e^{-jk2d}\} + \dots \quad (3.27)$$

where d is the thickness of the layer and k stands for k_2 (second medium). Then, as done for the previous case, the sound pressure can be expressed in the following form:

$$p^-(x) = a \sum_{i=0}^n b^i, \quad (3.28)$$

where:

$$a = P_{t12} r_{23} e^{jk_2(x-2d)} \quad \text{and} \quad b = r_{21} r_{23} e^{-jk_2 2d}. \quad (3.29)$$

The sum for this series is again

$$p^-(x) = a \left(\frac{1}{1-b} \right) \quad (3.30)$$

that, in terms of travelling waves, can be written as

$$p^-(x) = \frac{P_t t_{12} r_{23} e^{jk_2(x-2d)}}{1 - \{r_{21} r_{23} e^{-jk_2 2d}\}}. \quad (3.31)$$

This is equivalent to writing

$$p^-(x) = P_t t_{12} r_{23} e^{jk_2(x-d)} + p^-(x) \{r_{21} r_{23} e^{-jk_2 2d}\}. \quad (3.32)$$

The sound pressure complex amplitude of the sum of all *negative waves* inside the layer in $x = 0$, is then given by:

$$p^-(0^+) = \frac{P_t t_{12} r_{23} e^{-jk_2 2d}}{1 - r_{21} r_{23} e^{-jk_2 2d}}. \quad (3.33)$$

In the case of rigid backing the reflection coefficient at the right hand side interface, r_{23} , is equal to 1, and thus

$$p^-(0^+) = \frac{P_t t_{12} e^{-jk_2 2d}}{1 - r_{21} e^{-jk_2 2d}}. \quad (3.34)$$

3.3.3 Considerations on the reflection coefficient

As shown in Figure 3.7, the propagating waves are first transmitted through the layer and then reflected towards the first medium and are travelling in the same direction as the first reflections. By adding all the components coming out of medium 2 to the first reflections, the actual outgoing wave is obtained.

By summing the complex amplitudes of the second order reflection at $x = 0$, and multiplying it by the corresponding transmission coefficient t_{21} , the complex amplitude of the global second order wave, which is reflected back to the left hand side medium, can be derived.

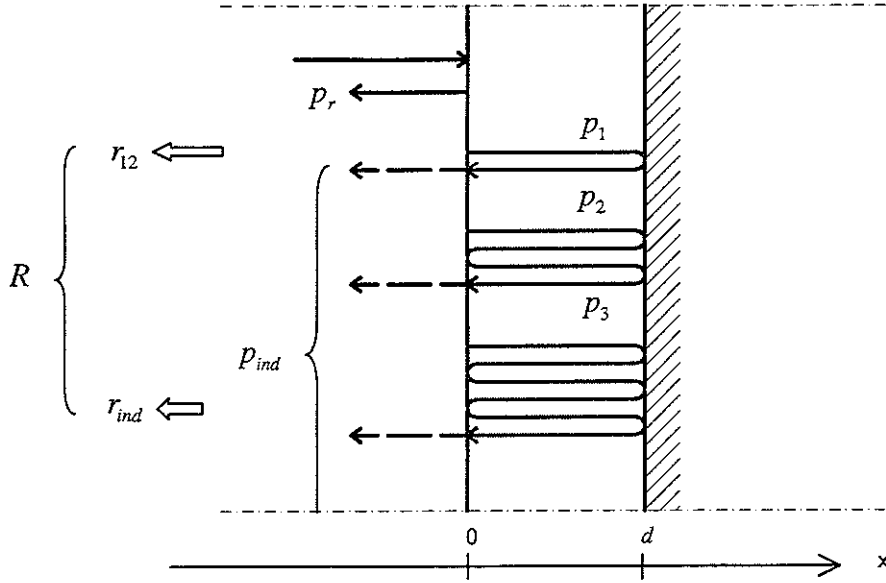


Figure 3.7 Schematization of the direct and indirect reflection processes for a layer with rigidly back right hand side

With reference to Figure 3.7, the sound pressures generated by the first three loops inside the layer are given by

$$p_1(0) = P_{t_{12}} e^{-jkd} r_{23} e^{-jkd} = P_{t_{12}} r_{23} e^{-jk2d} \quad (3.35)$$

$$p_2(0) = P_{t_{12}} r_{23} e^{-jk2d} \cdot r_{21} e^{-jkd} r_{23} e^{-jkd} = \{P_{t_{12}} r_{23} e^{-jk2d}\} \{r_{21} r_{23} e^{-jk2d}\} \quad (3.36)$$

$$p_3(0) = \{P_{t_{12}} r_{23} e^{-jk2d}\} \{r_{21} r_{23} e^{-jk2d}\} \{r_{21} r_{23} e^{-jk2d}\} \quad (3.37)$$

By induction, the sound pressure due to the n -th loop is then given by

$$p_n(0) = p_1(0) + p_2(0) + p_3(0) + \dots \quad (3.38)$$

so that, as previously discussed, it can be expressed in terms of a summation of the type

$$p(0^+) = a \sum_{i=0}^n b^i \quad (3.39)$$

where a and b are those defined by equations (3.29) .

The sum is therefore given by

$$p_{ind}(0^+) = p(0^+) = \frac{P_i t_{12} r_{23} e^{-jk_2 2d}}{1 - \{r_{21} r_{23} e^{-jk_2 2d}\}}. \quad (3.40)$$

It can be easily observed that this equation is identical to that for the sound pressure of the negative going waves at $x=0$.

It is now straightforward to obtain the complex amplitude of the wave on the left hand side of the layer interface, which is referred to as the indirect pressure p_{ind} , by simply multiplying it by the relative transmission coefficient t_{21} :

$$p_{ind}(0^-) = t_{21} p^-(0^+) = \frac{P_i t_{12} t_{21} r_{23} e^{-jk_2 2d}}{1 - \{r_{21} r_{23} e^{-jk_2 2d}\}}. \quad (3.41)$$

The total sound pressure in medium 1, sum of the interface and second order reflections, is given by

$$p_{tot}(x) = p_r(x) + p_{ind}(x) = (r_{12} + r_{ind}) P_{i0} e^{jk_1 x} = R P_{i0} e^{jk_1 x} \quad (3.42)$$

where total reflection coefficient R is given by

$$R = r_{12} + r_{ind} = r_{12} + \frac{t_{12} t_{21} r_{23} e^{-jk_2 2d}}{1 - \{r_{21} r_{23} e^{-jk_2 2d}\}} \quad (3.43)$$

and

$$r_{ind} = \frac{p_{ind}(0^-)}{P_{i0}}. \quad (3.44)$$

The reflection coefficient R obtained with this formulation, has been compared with that given by Kinsler *et al.* (2000):

$$R = \frac{\left(1 - \frac{z_1}{z_3}\right) \cos k_2 d + j \left(\frac{z_2}{z_3} - \frac{z_1}{z_2}\right) \sin k_2 d}{\left(1 + \frac{z_1}{z_3}\right) \cos k_2 d + j \left(\frac{z_2}{z_3} + \frac{z_1}{z_2}\right) \sin k_2 d}, \quad (3.45)$$

where the formula for the reflection coefficient has been derived from the conditions of continuity of the specific acoustic impedance at the boundaries between media 1 and 2 and then 2 and 3.

3.3.4 Representation of waves in a rigidly backed layer of porous material

Considering first the particular case of a rigidly backed layer with a fluid characterised by both real density and speed of sound, then the wave propagation and reflection are given in Figure 3.8. The two plots show the incident and reflected wave components and the standing wave in the layer with reference to the non-dimensional frequency (Brennan and To, 2001)

$$\Omega = \frac{\omega}{\omega_r} \quad (3.46)$$

where ω_r correspond to the ω_i defined for a porous material in Appendix C. It correspond to the frequency at which the mass-like behaviour of a porous material starts to dominate over the damping like behaviour. A detailed description of the parameters of the porous medium considered in the simulation is given in the same appendix. The presence of two discontinuity surfaces, i.e. the front face of the second medium and the rigid backing, creates the conditions for standing waves in the layer.

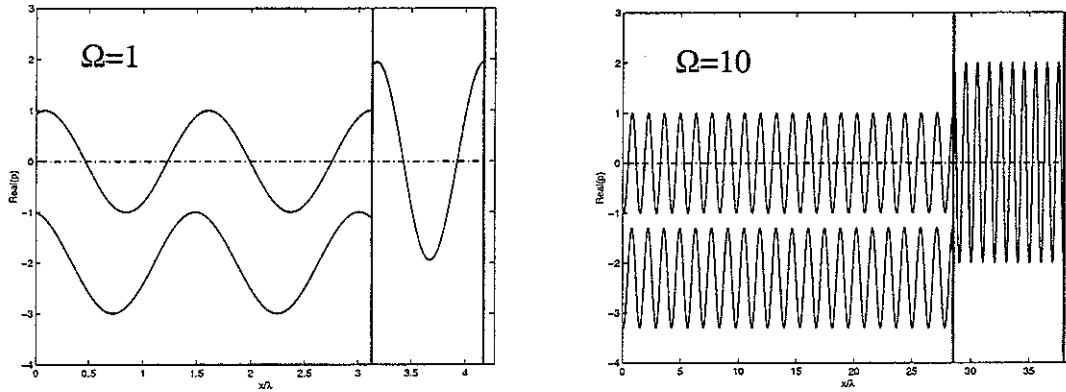


Figure 3.8 Incident, transmitted and reflected waves for a layer of fluid with rigid backing, characterised by real density, wavenumber, impedance and speed of sound for $\Omega=1$ (left) and $\Omega=10$ (right). The x axis normalised to the wavelength in the second medium

In Figure 3.9 and 3.10 examples are given, instead, for waves impinging on a layer of porous material for $\Omega = 10$ and $\Omega = 1$, respectively.

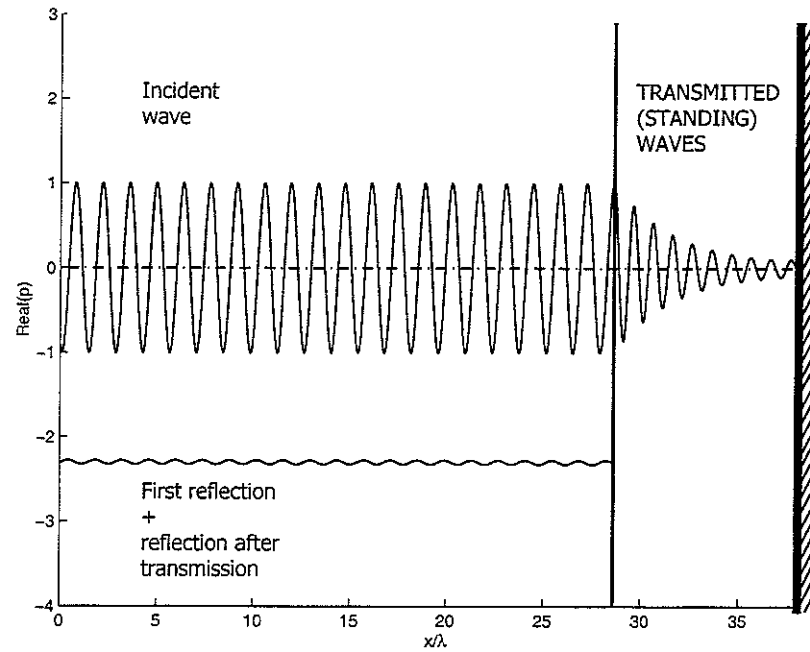


Figure 3.9 Incident, transmitted and reflected waves for a rigidly backed layer of porous material, whose properties are listed in Appendix C ($\Omega=10$)

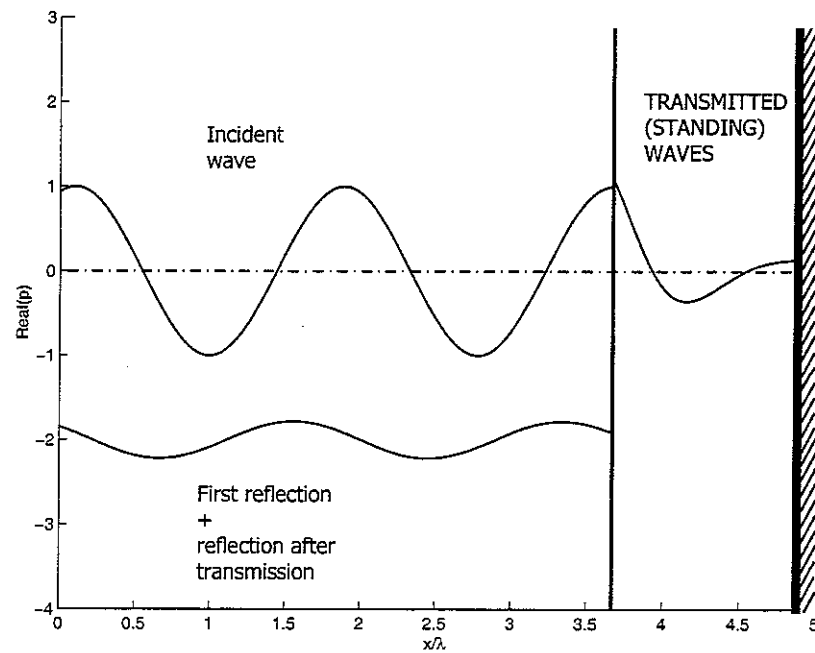


Figure 3.10 Incident, transmitted and reflected waves for a rigidly backed layer of porous material, whose properties are listed in Appendix C ($\Omega=1$)

3.4 Acoustic absorption

The relation derived for the reflection coefficient R of a rigidly backed layer can be used to evaluate the absorption coefficient for normal sound incidence, of the porous material through the equation (Kinsler *et al*, 2000):

$$A = 1 - |R|^2 \quad (3.47)$$

Figures 3.11 and 3.12 show four sets of plots for different values of the normalised thickness d/λ_i (1, 0.63, 0.21 and 0.1) of the porous layer with the incident, reflected and standing wave in the layer at $\Omega = 10$ (top plot), the real and imaginary components of the reflection coefficient for $10^{-2} < \Omega < 10^2$ (centre plot) and the absorption coefficient for the same frequency range. λ_i is the wavelength corresponding to the circular frequency ω_i , defined in Appendix C.

The dash dot lines stand for the semi-infinite porous material case, and they represent the asymptotic limit for large values of the thickness. What seems to be clear is that while going towards smaller values of the thickness, the reflection and absorption coefficient curves oscillates more and more, due to resonance phenomena. For higher frequencies, the absorption coefficient becomes constant, which is around 1 for large thicknesses. This value (from here on referred to as *absorption plateau*) reduces as the thickness decreases. It has to be noticed that for simplicity the values of the normalised thickness in the plots relate to the specific cases where the thickness of the material itself has a finite value.

Layer of porous material (complex density)
 $d/\lambda_t = 1, \Omega = 10$

Layer of porous material (complex density)
 $d/\lambda_t = 0.63, \Omega = 10$

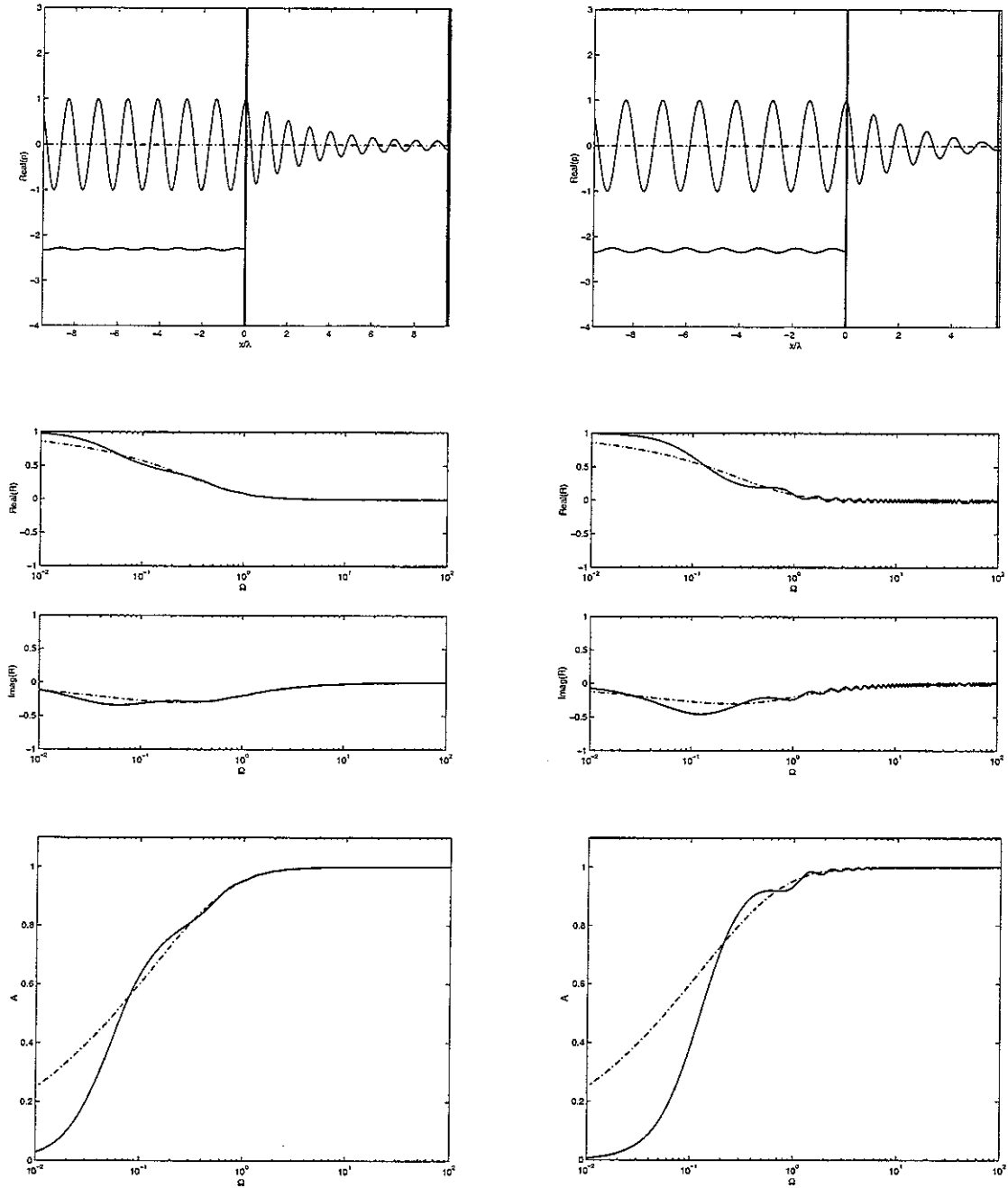


Figure 3.11 Sound pressure of the incident and reflected waves and of the standing wave in the layer for $\Omega=10$ (top plots – x - axis normalised to the wavelength on the second medium), real and imaginary parts of the reflection coefficient (centre plot) and absorption coefficient (bottom plot). Solid line: layer of finite thickness $d/\lambda_t=1$ (left column) and $d/\lambda_t=0.63$ (right column). Dashed line: semi-infinite porous material. Values of the normalised thickness relate to specific cases where the thickness of the material itself has a finite value

Layer of porous material (complex density)
 $d/\lambda_t=0.21, \Omega=10$

Layer of porous material (complex density)
 $d/\lambda_t=0.1, \Omega=10$

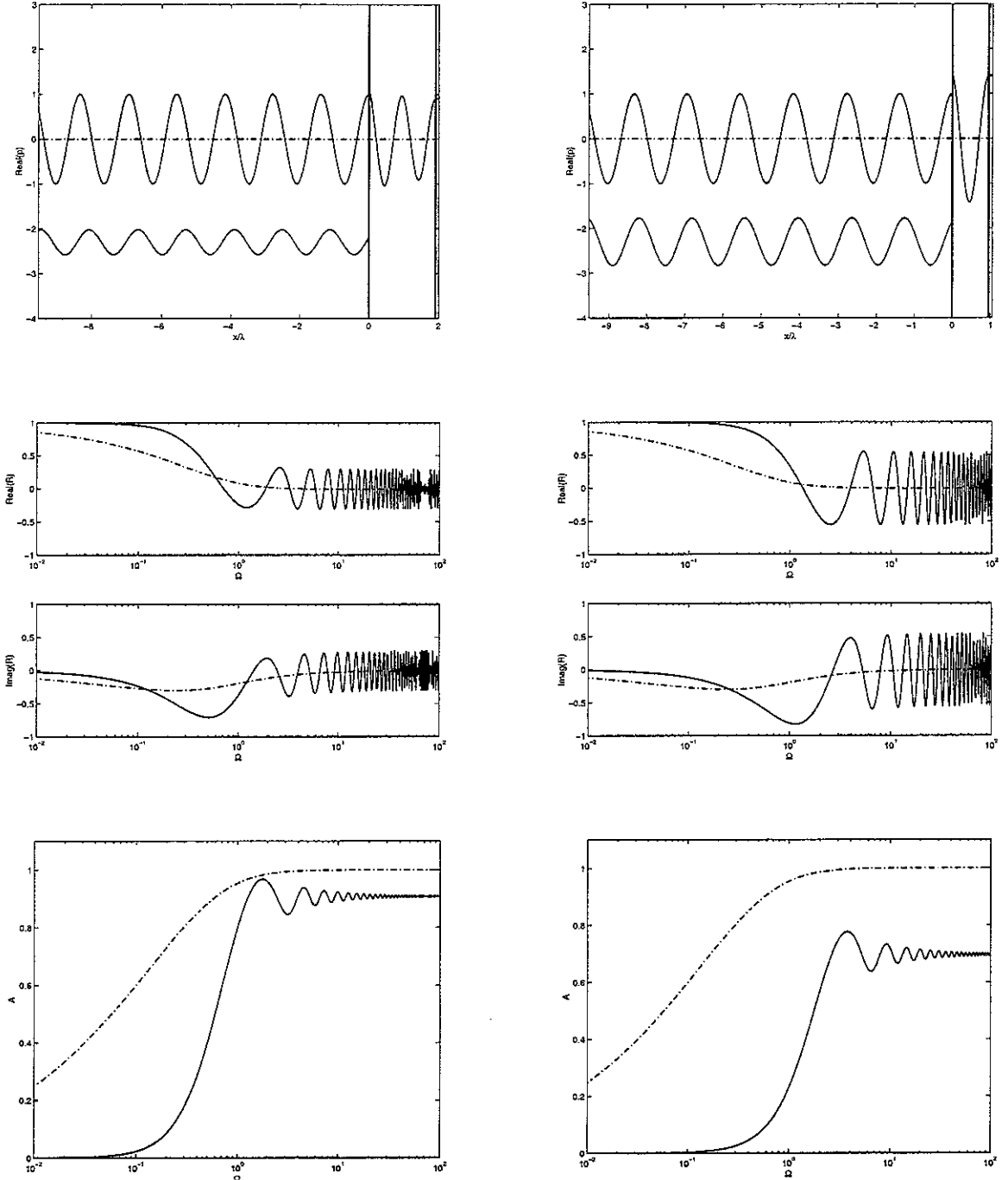


Figure 3.12 Sound pressure of the incident and reflected waves and of the standing wave in the layer for $\Omega=10$ (top plots – x -axis normalised to the wavelength on the second medium), real and imaginary parts of the reflection coefficient (centre plot) and absorption coefficient (bottom plot). Solid line: layer of finite thickness $d/\lambda_t = 0.21$ (left column) and $d/\lambda_t = 0.1$ (right column). Dashed line: semi-infinite porous material. Values of the normalised thickness relate to specific cases where the thickness of the material itself has a finite value l

3.5 Absorption and transmission of a layer of porous material without rigid backing

As shown in Figure 3.13, if the layer under study is without any rigid backing, there is also a transmitted wave in the third medium.

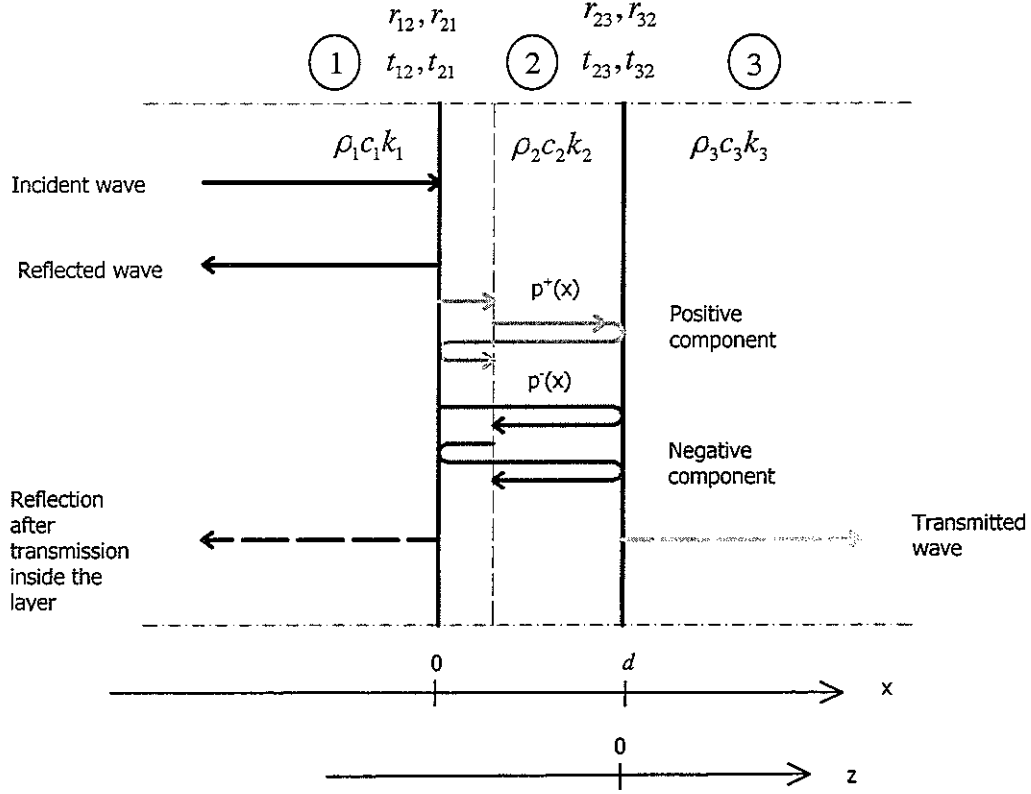


Figure 3.13 Schematization of reflected and transmitted waves for a finite thickness layer of porous material, with no rigid backing

Positive and negative components in the second medium are expressed by the equations seen in § 3.3.1 and § 3.3.2. The actual sound pressure amplitudes will be reduced due to the transmission of sound energy to the third medium. In order to derive the transmitted wave in the third medium, the sound pressure at $x = d$ needs to be derived. In a similar way as for the wave retransmitted in the first medium (Figure 3.7), the sound pressure of this wave can be derived by evaluating the sound pressure of the positive component at $x = d$ (see Figure 3.13), and then multiplying it by t_{23} , as follows

$$p^+(d^+) = t_{23} p^+(d^-) = \frac{P t_{12} t_{23} e^{-jk_2 d}}{1 - \{r_{21} r_{23} e^{-jk_2 2d}\}} \quad (3.48)$$

Thus, considering for simplicity a new reference system with a z -axis with the origin in $x = d$ (see Figure 3.14) the expression for the outgoing wave (after transmission through the layer) is:

$$p_t(z) = \frac{P_i t_{12} t_{23} e^{-jk_2 d}}{1 - \{r_{21} r_{23} e^{-jk_2 2d}\}} \cdot e^{-jk_3 z} \quad (3.49)$$

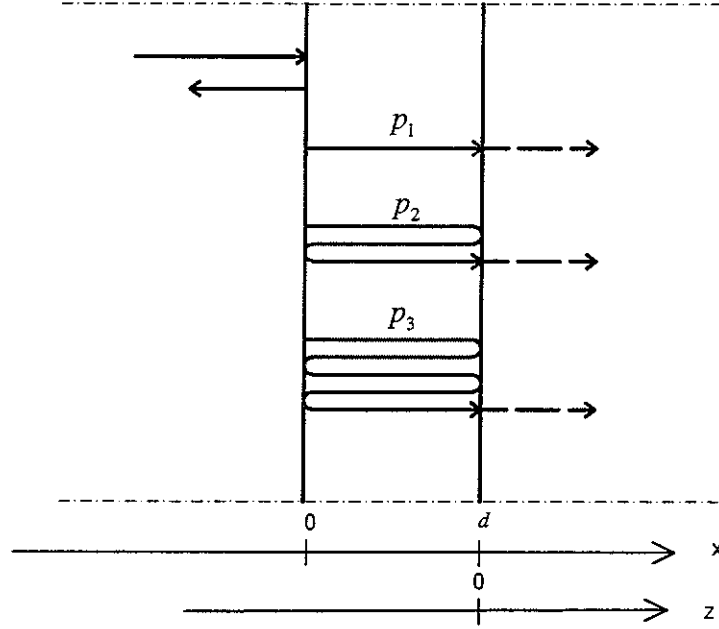


Figure 3.14 Schematization of reflected and transmitted waves for a finite thickness layer of porous material with no rigid backing

Figures 3.15 and 3.16 show the same plots given in Figures 3.11 and 3.12 for a layer of absorption material without rigid backing. The dash dot line represents again the reference limit case of a semi-infinite porous material, while the solid line represents the case of transmission through the layer, with normalised thickness 1, 0.63, 0.21 and 0.1. The x -axis in the graphs is normalized to the wavelength λ_2 of the sound inside the layer. It can be noticed that at high frequencies the limiting value for the absorption coefficient is 1 for every thickness of the layer, but differences can be observed at low frequency, where the absorption seems to be inversely proportional to the thickness of the layer. In this case the sound energy is not only dissipated inside the layer, but it also travels through the layer. Besides this, lower frequency means greater wavelength, and if the incident waves impinge upon a thick layer, it is more likely for them to be reflected rather than to be transmitted, and vice versa for a thin layer. In the case of rigid backing reflections from the wall can be also retransmitted again in medium 1.

An extension of this work results in the definition of a transmission coefficient T as previously pointed out and shown in Figure 3.5:

$$T = \frac{P_t}{P_i} = \frac{p_t(0)}{P_i} = \frac{1}{P_i} \cdot \frac{P_i t_{12} t_{23} e^{-jk_2 d}}{1 - r_{21} r_{23} e^{-jk_2 2d}} \quad (3.50)$$

where P_i is intended to be the amplitude of the wave in medium 3 at $z = 0$ or $x = d$.

Layer of porous material with no rigid backing
 $d/\lambda_t=1, \Omega=10$

Layer of porous material with no rigid backing
 $d/\lambda_t=0.63, \Omega=10$

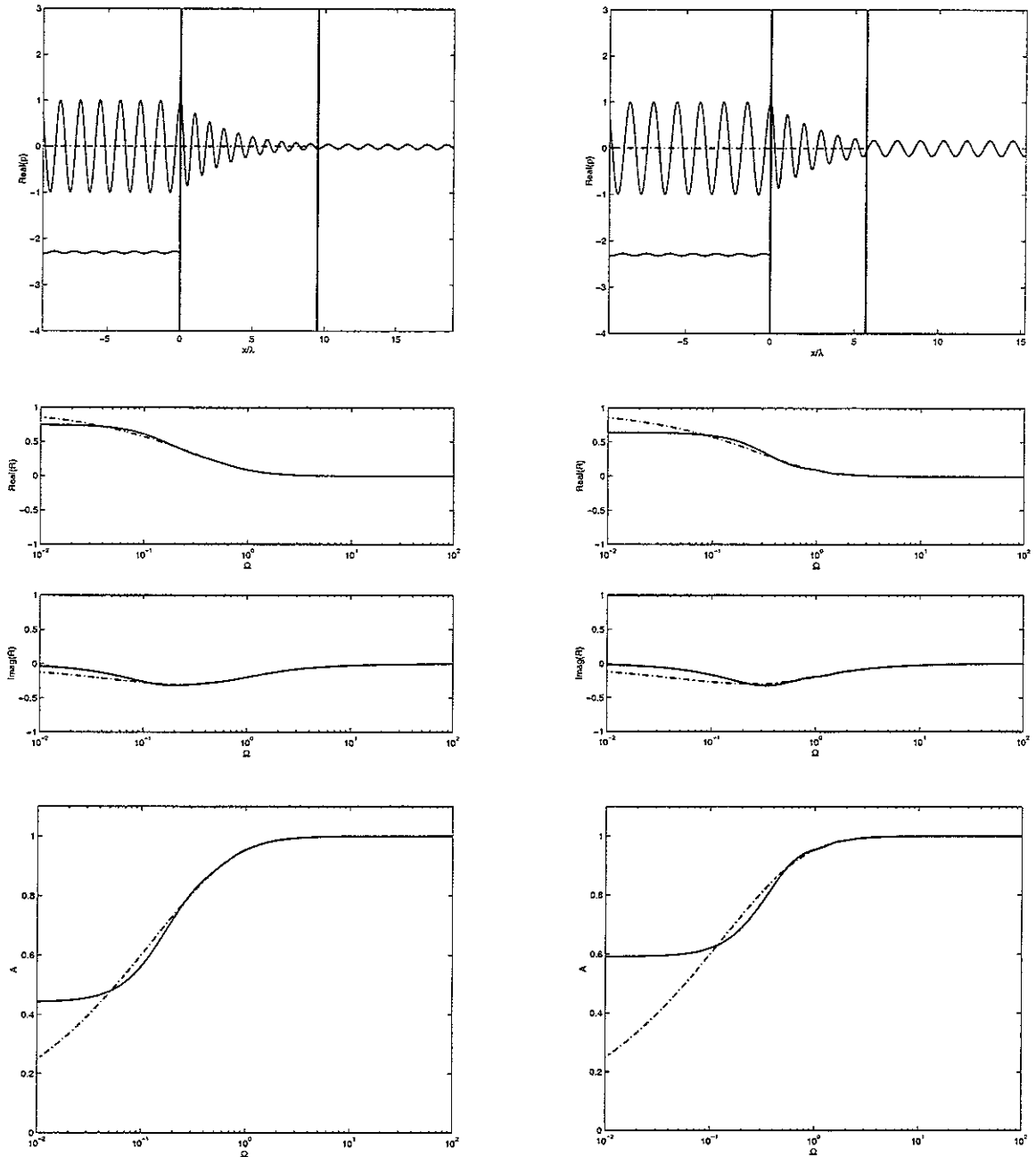


Figure 3.15 Sound pressure of the incident, reflected, transmitted waves and of the standing wave in the layer for $\Omega=10$ (top plots – x - axis normalised to the wavelength on the second medium), real and imaginary parts of the reflection coefficient (centre plot) and absorption coefficient (bottom plot). Solid line: layer of finite thickness $d/\lambda_t=1$ (left column) and $d/\lambda_t=0.63$ (right column) with no rigid backing. Dash-dotted line: semi-infinite porous material

Layer of porous material with no rigid backing
 $d/\lambda_t=0.21$, $\Omega=10$

Layer of porous material with no rigid backing
 $d/\lambda_t=0.1$, $\Omega=10$

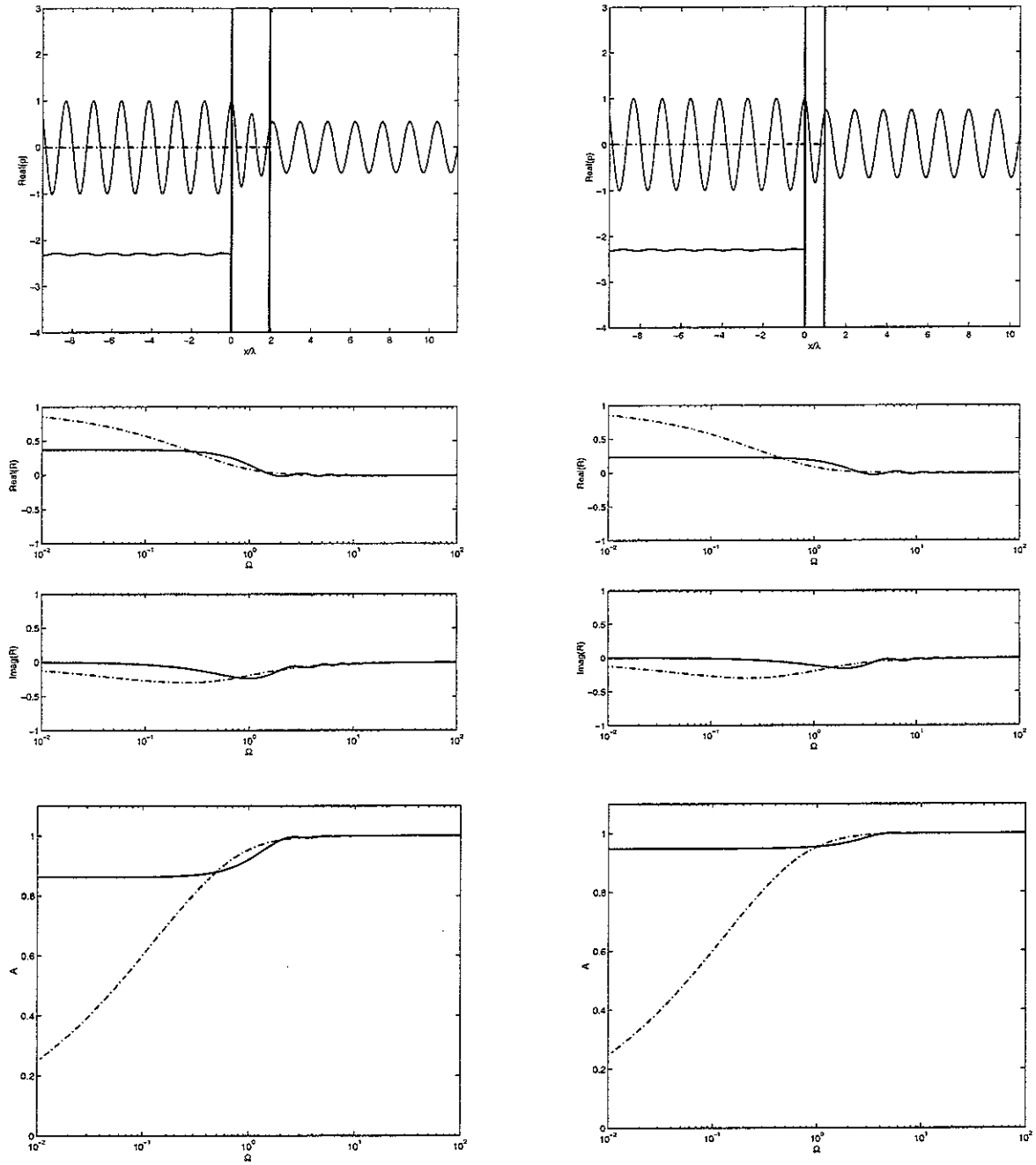


Figure 3.16 Sound pressure of the incident, reflected, transmitted waves and of the standing wave in the layer for $\Omega=10$ (top plots – x - axis normalised to the wavelength on the second medium), real and imaginary parts of the reflection coefficient (centre plot) and absorption coefficient (bottom plot). Solid line: layer of finite thickness $d/\lambda_t=0.21$ (left column) and $d/\lambda_t=0.1$ (right column) with no rigid backing. Dash-dotted line: semi-infinite porous material

3.6 Absorption of a porous layer at a certain distance from a rigid wall

In the case where the layer of porous material is not fixed over a rigid backing, but is placed instead at a certain distance from it, a standing wave is generated also in the air gap between the porous medium and the rigid backing. After transmission back again in the porous layer, a new component arises in medium 1 and again it has to be summed with the first reflection and the “second order” reflection component, arising from the standing wave in the porous medium. In this case the *reflection coefficient* R has thus a new component.

3.6.1 Waves in the air gap between the porous material and the rigid backing

A representation of the system with a layer placed at a certain distance from a rigid wall is given in Figure 3.17.

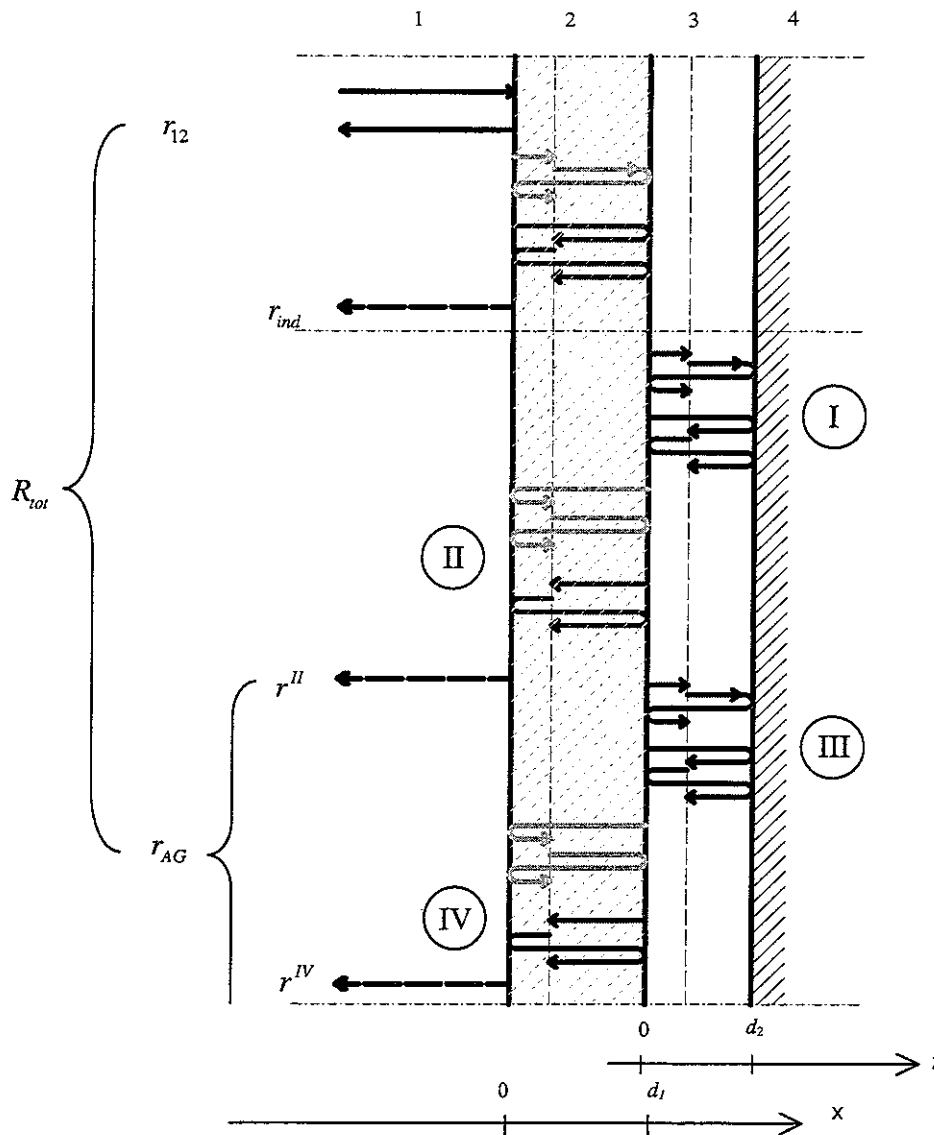


Figure 3.17 Schematisation of a layer of porous material of thickness d_1 placed at a distance d_2 from a rigid wall

The expressions for the positive and negative going wave components in the air cavity between the layer and the rigid wall can be derived from eq. (3.22) and (3.31) respectively, bearing in mind that the incident wave relative to the cavity has obviously a different complex amplitude as compared to the original incident wave P_i . The various components will be indexed with reference to the notation shown in Figure 3.15. As in § 3.5, two reference systems will be used (x and z variables). For the waves in the cavity then

$$p^{I+}(z) = \frac{P_i^I t_{23} e^{-jk_3 z}}{1 - \{r_{32} r_{34} e^{-jk_3 2d_2}\}}, \quad (3.51)$$

$$p^{I-}(z) = \frac{P_i^I t_{23} r_{34} e^{jk_3(z-2d_2)}}{1 - \{r_{32} r_{34} e^{-jk_3 2d_2}\}}, \quad (3.52)$$

where $P_i^I = p^+(d^-)$ is the complex amplitude in $x = d^-$ and $t_{23} P_i^I$ is the actual complex amplitude of the incident wave for the waves of index I (amplitude in $x = d^+$). The expression for the sound pressure in the cavity is thus

$$p^{I_{tot}}(z) = p^{I+}(z) + p^{I-}(z). \quad (3.53)$$

If the waves retransmitted in medium 2 are now considered (index II in Figure 3.17), then the positive going wave component can be written as

$$\begin{aligned} p^{II+}(x) = & P_i^{II} t_{32} e^{-jk_2 d} r_{21} e^{-jk_2 x} + \{P_i^{II} t_{32} e^{-jk_2 d} r_{21} e^{-jk_2 x}\} \{e^{-jk_2(d-x)} r_{23} e^{-jk_2 d} r_{21} e^{-jk_2 x}\} + \\ & + \{P_i^{II} t_{32} e^{-jk_2 d} r_{21} e^{-jk_2 x}\} \{e^{-jk_2(d-x)} r_{23} e^{-jk_2 d} r_{21} e^{-jk_2 x}\} \{e^{-jk_2(d-x)} r_{23} e^{-jk_2 d} r_{21} e^{-jk_2 x}\} + \dots \end{aligned} \quad (3.54)$$

which corresponds to:

$$\begin{aligned} p^{II+}(x) = & P_i^{II} t_{32} r_{21} e^{-jk_2(x+d)} + \{P_i^{II} t_{32} r_{21} e^{-jk_2(x+d)}\} \{r_{21} r_{23} e^{-jk_2 2d}\} + \\ & + \{P_i^{II} t_{32} r_{21} e^{-jk_2(x+d)}\} \{r_{21} r_{23} e^{-jk_2 2d}\} \{r_{21} r_{23} e^{-jk_2 2d}\} + \dots \end{aligned} \quad (3.55)$$

and then, using the same formula for the series summation of eq. (3.39),

$$p^{\text{II}+}(x) = \frac{P_i^{\text{II}} t_{32} r_{21} e^{-jk_2(x+d)}}{(1 - r_{21} r_{23} e^{-jk_2 2d})} \quad (3.56)$$

where

$$P_i^{\text{II}} = p^{\text{I}-}(0^+) = \frac{P_i^{\text{I}} r_{34} e^{-jk_3 2d_2}}{1 - \{r_{32} r_{34} e^{-jk_3 2d_2}\}} \quad (3.57)$$

In the same way, the negative going wave component can be written as

$$\begin{aligned} p^{\text{II}-}(x) = & P_i^{\text{II}} t_{32} e^{jk_2(x-d)} + \{P_i^{\text{II}} t_{32} e^{jk_2(x-d)}\} \{e^{-jk_2 x} r_{21} e^{-jk_2 d} r_{23} e^{-jk_2(x-d)}\} + \\ & + \{P_i^{\text{II}} t_{32} e^{jk_2(x-d)}\} \{e^{-jk_2 x} r_{21} e^{-jk_2 d} r_{23} e^{-jk_2(x-d)}\} \{e^{-jk_2 x} r_{21} e^{-jk_2 d} r_{23} e^{-jk_2(x-d)}\} + \dots \end{aligned} \quad (3.58)$$

and

$$\begin{aligned} p^{\text{II}-}(x) = & P_i^{\text{II}} t_{32} e^{jk_2(x-d)} + \{P_i^{\text{II}} t_{32} e^{jk_2(x-d)}\} \{r_{21} r_{23} e^{-jk_2 2d}\} + \\ & + \{P_i^{\text{II}} t_{32} e^{jk_2(x-d)}\} \{r_{21} r_{23} e^{-jk_2 2d}\} \{r_{21} r_{23} e^{-jk_2 2d}\} + \dots, \end{aligned} \quad (3.59)$$

which becomes

$$p^{\text{II}-}(x) = \frac{P_i^{\text{II}} t_{32} e^{jk_2(x-d)}}{1 - \{r_{21} r_{23} e^{-jk_2 2d}\}}. \quad (3.60)$$

The same method is applied to derive expressions for the waves with index III and IV in Figure 3.17, so that

$$p^{\text{III}+}(z) = \frac{P_i^{\text{III}} t_{23} e^{-jk_3 z}}{1 - \{r_{32} r_{34} e^{-jk_3 2d_2}\}}, \quad (3.61)$$

$$p^{\text{III}-}(z) = \frac{P_i^{\text{III}} t_{23} r_{34} e^{jk_3(z-2d_2)}}{1 - \{r_{32} r_{34} e^{-jk_3 2d_2}\}}, \quad (3.62)$$

where $P_i^{\text{III}} = p^{\text{II}+}(d^-)$ and for the IV index waves

$$p^{\text{IV}+}(x) = \frac{P_i^{\text{IV}} t_{32} r_{21} e^{-jk_2(x+d)}}{1 - \{r_{21} r_{23} e^{-jk_2 2d}\}} \quad (3.63)$$

$$P_i^{IV-}(x) = \frac{P_i^{IV} t_{32} e^{jk_2(x-d)}}{1 - \{r_{21} r_{23} e^{-jk_2 2d}\}} \quad (3.64)$$

where $P_i^{IV} = P_i^{III-}(0^+)$. It is now possible to define an additional component for the reflection coefficient due to transmission towards the medium one from the standing wave II as shown in Figure 3.17

$$r^{II} = \frac{P_i^{II}(0^+) t_{21}}{P_i} = \frac{t_{12} t_{21} t_{23} t_{32} r_{34} e^{-jk_2 2d} e^{-jk_3 2d_2}}{(1 - r_{21} r_{23} e^{-jk_2 2d})^2 (1 - r_{32} r_{34} e^{-jk_3 2d_2})}. \quad (3.65)$$

This reflection coefficient is representative only of the second group of reflections. By referring now to the waves indexed as IV, the coefficient r^{IV} can be derived

$$r^{IV} = \frac{P_i^{IV}(0^-) t_{21}}{P_i} = \frac{t_{12} t_{21} t_{23}^2 t_{32}^2 r_{21} r_{34}^2 e^{-jk_2 4d} e^{-jk_3 4d_2}}{(1 - r_{21} r_{23} e^{-jk_2 2d})^3 (1 - r_{32} r_{34} e^{-jk_3 2d_2})^2} \quad (3.66)$$

which can also be written as

$$r^{IV} = \frac{t_{12} t_{21} t_{23} t_{32} r_{34} e^{-jk_2 2d} e^{-jk_3 2d_2}}{(1 - r_{21} r_{23} e^{-jk_2 2d})^2 (1 - r_{32} r_{34} e^{-jk_3 2d_2})} \cdot \frac{t_{23} t_{32} r_{21} r_{34} e^{-jk_2 2d} e^{-jk_3 2d_2}}{(1 - r_{21} r_{23} e^{-jk_2 2d}) (1 - r_{32} r_{34} e^{-jk_3 2d_2})}. \quad (3.67)$$

It may be noticed that the first factor in eq. (3.67) is equal to r^{II} . By extending this procedure to higher order reflection-transmission effects within and between the two layers, the higher order terms in the series for the reflection terms r^{II} and r^{IV} are found. The sum for these two series is the same as in the previous cases

$$r_{AirGap} = a \left(\frac{1}{1-b} \right), \quad (3.68)$$

where, in this case,

$$a = \frac{t_{12} t_{21} t_{23} t_{32} r_{34} e^{-jk_2 2d} e^{-jk_3 2d_2}}{(1 - r_{21} r_{23} e^{-jk_2 2d})^2 (1 - r_{32} r_{34} e^{-jk_3 2d_2})} \quad (3.69a)$$

$$b = \frac{t_{23} t_{32} r_{21} r_{34} e^{-jk_2 2d} e^{-jk_3 2d_2}}{(1 - r_{21} r_{23} e^{-jk_2 2d}) (1 - r_{32} r_{34} e^{-jk_3 2d_2})}. \quad (3.69b)$$

In conclusion, the reflection coefficient due to the propagation of acoustic waves in the layer of porous material and in the air gap is given by

$$r_{AG} = r^{II} + r^{IV} + \dots = \frac{\frac{t_{12}t_{21}t_{23}t_{32}r_{34}e^{-jk_2 2d}e^{-jk_3 2d_2}}{(1-r_{21}r_{23}e^{-jk_2 2d})^2(1-r_{32}r_{34}e^{-jk_3 2d_2})}}{1 - \frac{t_{23}t_{32}r_{21}r_{34}e^{-jk_2 2d}e^{-jk_3 2d_2}}{(1-r_{21}r_{23}e^{-jk_2 2d})(1-r_{32}r_{34}e^{-jk_3 2d_2})}} \quad (3.70.a)$$

or

$$r_{AG} = \frac{t_1 e^{-j2(k_2 d + k_3 d_2)}}{(1-r_1 e^{-jk_2 2d})(1-r_2 e^{-jk_3 2d_2}) - (1-r_1 e^{-jk_2 2d})t_2 e^{-j2(k_2 d + k_3 d_2)}} \quad (3.70.b)$$

The total reflection coefficient is now given by the sum of the previously derived ones, r_{ind} and r_{AG} , and the first reflection one r_{12}

$$R_{tot} = r_{12} + r_{ind} + r_{AG} \quad (3.71)$$

This reflection coefficient can be used to evaluate the absorption coefficient of a layer of porous material placed at a certain distance from a rigid wall, according to eq. (3.47). In Figure 3.18 a few plots are given of the absorption coefficient for different values of the thickness of the layer and of the cavity depth. The absorption coefficient

$$A_{tot} = 1 - |R_{tot}|^2 \quad (3.72)$$

is represented (thin line), together with the reference semi-infinite case (dash dotted line), and the case of rigid backing (thick line). Figures 3.18 a) and 3.18 b) refer to different values of the normalised thickness $d/(\lambda_i/4)$. For a given thickness of a porous layer, the introduction of an air gap with the rigid backing does slightly improve the low frequency absorption but it also increases the low frequency oscillation of the absorption due to resonant effects. It can be seen that the height of the absorption plateau is only dependent on the thickness of the porous layer.

The frequency values at which minima of absorption occur are connected with the total thickness of layer and cavity depth and the acoustic wavelength as shown in Figure 3.19 and Table 3.1.

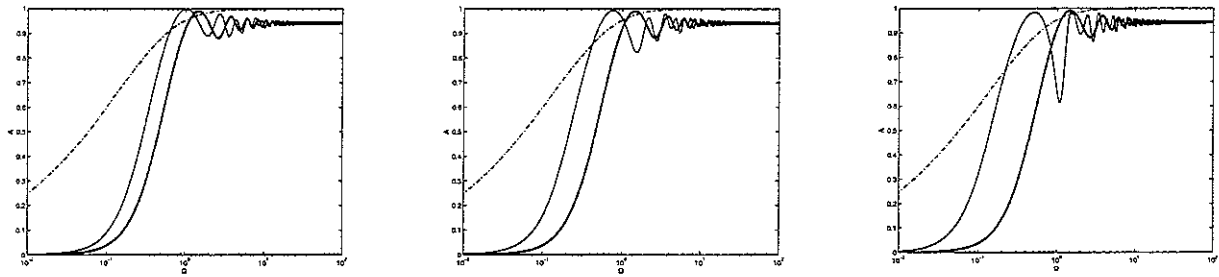


Figure 3.18 a) Absorption coefficient curves for $d_n = d/(\lambda_1/4) = 1$ and three different values of d_2/d_1 (0.05; 1; 2)-thick line; reference rigid backing case-thin line; semi-infinite case – das dotted line

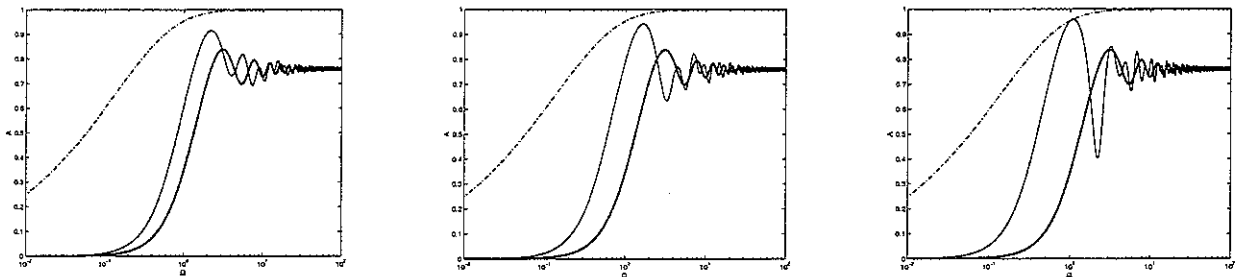


Figure 3.18 b) Absorption coefficient curves for $d_n = d/(\lambda_1/4) = 0.5$ and three different values of d_2/d_1 (0.05; 1; 2)-thick line; reference rigid backing case-thin line

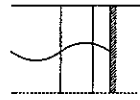
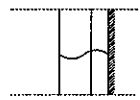
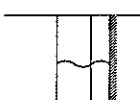
			Calculus	graph
Ω_1	$\lambda_1 = (d_1 + d_2) * 2$		1.04	1.08
Ω_2	$\lambda_2 = \lambda_1 / 2$		2.08	2.16
Ω_3	$\lambda_3 = \lambda_1 / 3$		3.12	3.23

Table 3.1 Comparison between the values for the non-dimensional frequencies Ω at which minima occur (deduced from the graph below) and the ones calculated with the reference acoustic wavelengths λ_1, λ_2 and λ_3 (wavelengths for which the amplitude is zero at the front surface of the layer)

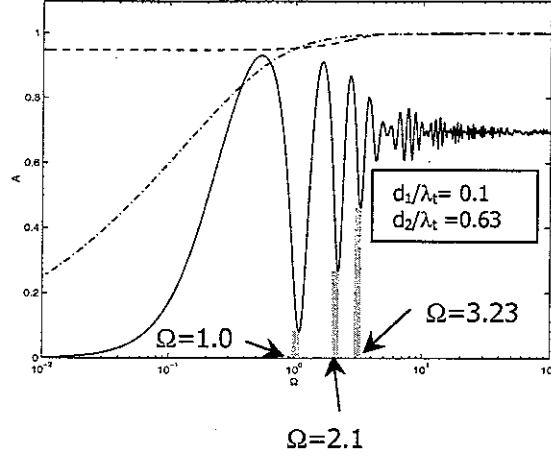


Figure 3.19 Frequencies of minimum absorption ($d_1/\lambda_t=0.1$ and $d_2/\lambda_t=0.63$)

3.6.2 Plateau height

For both the rigid backing and the air gap case, the absorption at high frequencies oscillates around a constant value (plateau). The curves shown in Figure 3.20 represent the values of the plateau against the normalised thickness for different values of the normalised cavity depth d_2/d_{\max} , where d_{\max} is the maximum value considered corresponding to 20 cm.

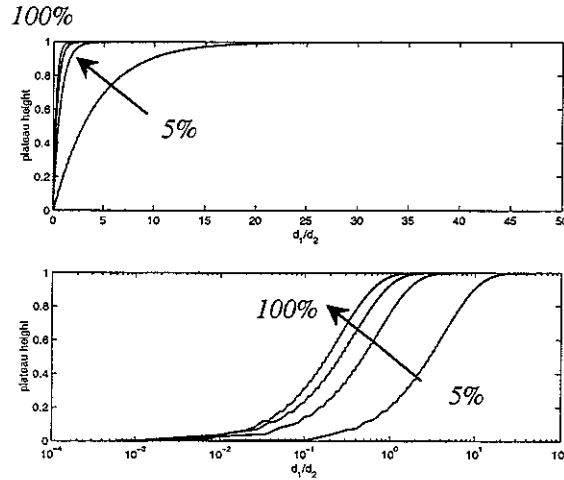


Figure 3.20 Plateau height plotted against the normalised thickness d_1/d_2 , for different values of the normalised cavity depth. $d_2/d_{\max} = 5\%$, 30% , 55% and 100% (linear and logarithmic scales)

All the curves presented so far concerning the plateau and the absorption coefficient are based on simplified formulae for the normalised acoustic impedance and wavenumber (see appendix C). Using these formulae allows for simple calculations, but can bring to underestimation of the damping of the material.

Figure 3.21 shows the real and imaginary parts of the effective density, defined as (Brennan and To, 2001)

$$\frac{\rho_e}{\rho_0 \alpha_\infty} = \left(1 + \frac{1}{j\Omega} \left(1 + j\Omega \frac{M}{2} \right)^{\frac{1}{2}} \right) \quad (3.73)$$

for increasing values of $M = \frac{8\alpha_\infty k_0}{h\Lambda^2}$, where α_∞ is the tortuosity, k_0 is the viscous permeability, h the porosity and Λ is the characteristic viscous dimension (see also Johnson *et al.* 1987).

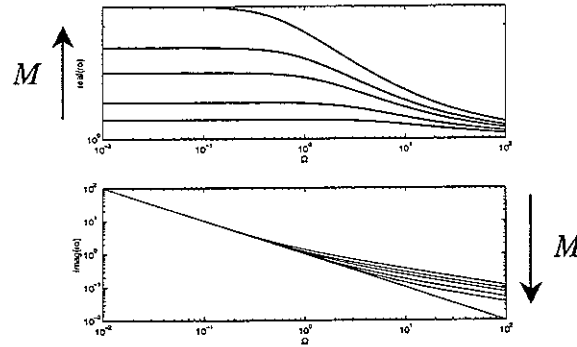


Figure 3.21 Real and imaginary parts of the effective density for increasing values of M , rigid backing case

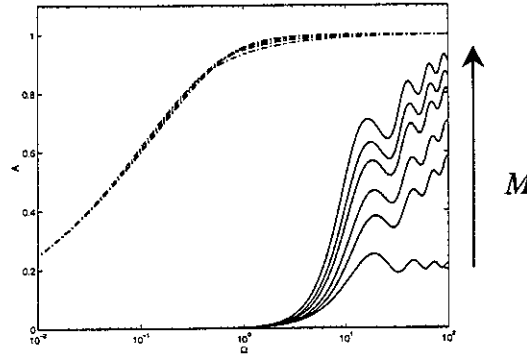


Figure 3.22 a) Absorption coefficient curves for increasing values of M (0; 0.5; 1; 2; 3; 5 respectively) and for $d_n=d/\lambda_t=0.02$. The curve with the plateau corresponds to $M=0$; rigid backing case

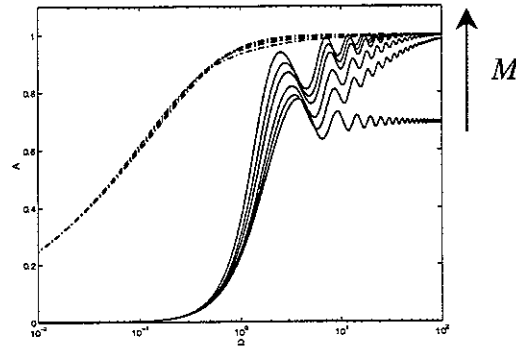


Figure 3.22 b) Absorption coefficient curves for increasing values of M (0; 0.5; 1; 2; 3; 5 respectively) and for $d_n=d/\lambda_t=0.1$. The curve with the plateau corresponds to $M=0$; rigid backing case

The curves of the imaginary part can be considerably different in the high frequencies region for values of M greater than zero. The damping effect of the porous medium is thus not negligible as compared to the mass of the system and the absorption coefficient can be remarkably increased in the same frequency region, as shown in Figures 3.22 a) and 3.22 b) for the rigid backing case. The absorption curves plotted so far all refer to the simple case of M equal to zero and represent a lower limit case for the general behaviour of rigid frame porous media.

Figure 3.23 a) and 3.23 b) shows equivalent plots for the case of an existing air gap and for values of M greater than 0, where d_n is the normalised thickness of the layer and D_n is the normalised sum of the thickness of the layer and the cavity depth.

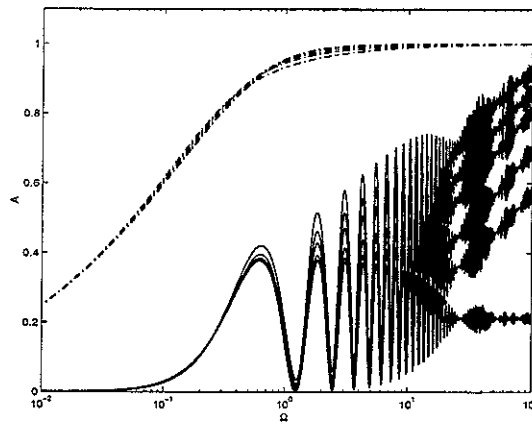


Figure 3.23 a) Absorption coefficient curves for increasing values of M (0; 0.5; 1; 2; 3; 5 respectively) and for $d_n=d/\lambda_r=0.033$ and $D_n=0.63$; air gap case

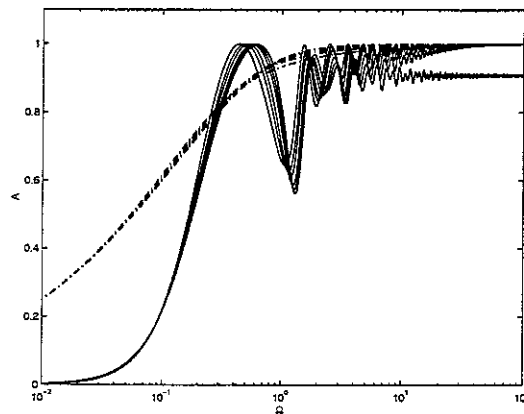


Figure 3.23 b) Absorption coefficient curves for increasing values of M (0; 0.5; 1; 2; 3; 5 respectively) and for $d_n=d/\lambda_r=0.33$ and $D_n=0.63$, air gap case

3.6.3 Peaks of absorption

An interesting analysis can also be done on the frequencies at which the first peak of absorption occur while varying the thickness of the layer or the cavity depth. This analysis has been done both for the case of rigid backing and of air gap between the layer and the rigid wall.

Figure 3.24 shows plots of absorption for the rigid backing case and for different values of d_1 , which is the thickness of the layer. Figure 3.25 shows instead the plots of absorption for the case with fixed value of d_2 (air gap), for different values of d_1 .

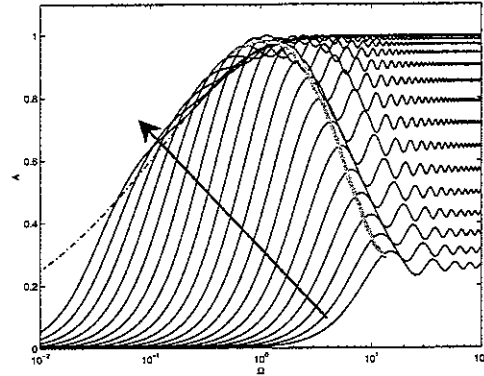


Figure 3.24 Absorption curves for different values of the thickness of the porous layer. Rigid backing case

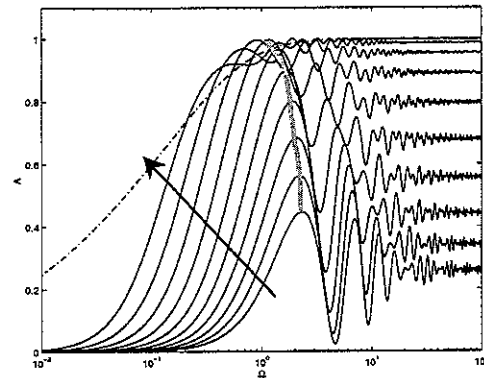


Figure 3.25 Absorption curves for different values of the thickness of the porous layer. Layer at a fixed distance from a rigid backing

Analytical expressions have also been derived for the resonance frequencies in the cases of rigid backing and air gap. It has been found that in the general case of separation between two layers of air, the peaks occur at frequencies for which the thickness of the second layer (rigid backing case) or the value of D (air gap case) equals the quarter wavelength of the standing wave inside the second layer, so that

$$\omega_{peak\,RB} = \frac{\pi}{2} \cdot \frac{c}{d} \quad \text{and} \quad \omega_{peak\,AG} = \frac{\pi}{2} \cdot \frac{c}{(d_1 + d_2)} \quad (3.74)$$

where $\omega_{peak\,RB}$ and $\omega_{peak\,AG}$ are the circular frequencies for peaks of absorption respectively for the two cases examined (RB stands for rigid backing case and AG for air gap case) and c is the speed of sound in air.

In other words the phase speed in the porous medium is always less than the free wave speed and this feature has a vital influence on sound absorption by porous sheets mounted on a reflective surface, because they exhibit absorption maxima and minima at the acoustic resonance and antiresonance frequencies, which correspond respectively to odd multiples of one quarter wavelength and multiples of one half wavelength of the sound propagating within the porous material.

For a given total thickness $D = d_1 + d_2$, the absorption increases with the thickness of the porous layer and the highest absorption is given for $d_1 = D$ and $d_2 = 0$, i.e. by occupying all the thickness D with porous material (limit case of simple rigid backing).

It can be noticed (see Figure 3.26) that when D is fixed, the peak frequency $\Omega_{peak\ AG}$ is practically constant, whereas for the case of fixed d_2 it tends to move towards smaller values for greater values of d_1 . It can also be noticed that the higher curve (limit case of zero cavity depth) assumes the same shape as the curves for the rigid backing case ($d_1 = D, d_2 = 0$).

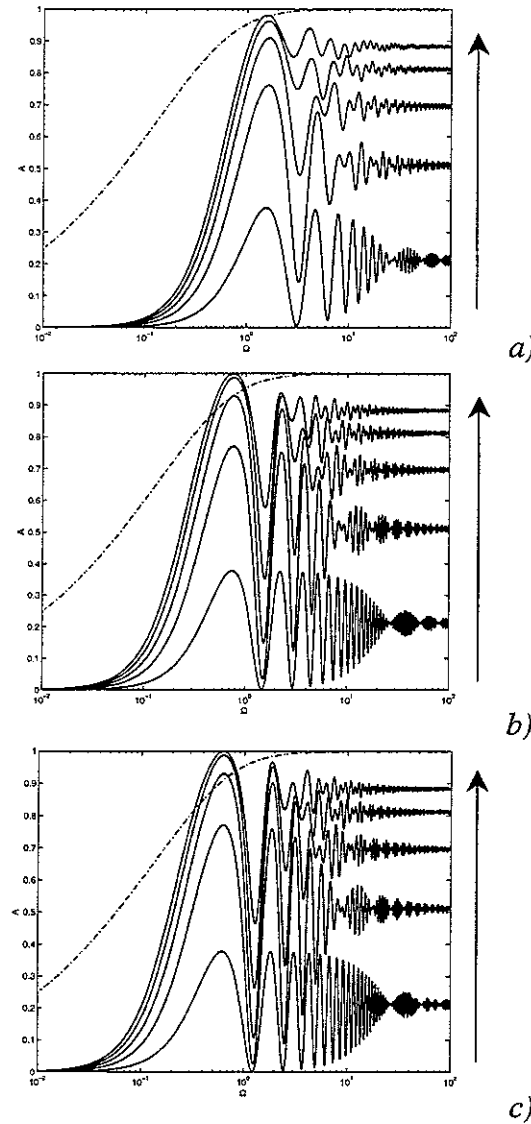


Figure 3.26. Absorption curves for different values of $D_n = D/\lambda_t$: a) $D_n = 0.25$; b) $D_n = 0.52$; c) $D_n = 0.63$.
Different curves in the same plot refer to different values of the normalised thickness $d_1/(\lambda_t/4)$

Finally, in order to compare the overall absorption provided by a rigidly backed layer with the one provided by the case with air gap, integration of the absorption curves has been done over the range of frequency $10^{-2} < \Omega < 10^2$ and the result is plotted in Figure 3.27. The difference between the two curves, which have been normalised to the integral of the semi-infinite case, can be seen only for really low values of d_1 . The integral curve for the air gap case remains practically the same when varying d_2 .

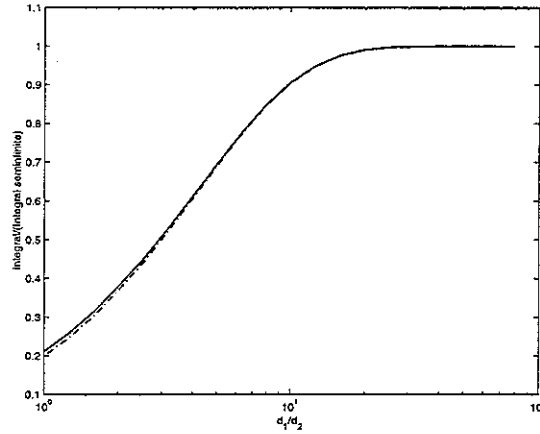


Figure 3.27. Integrated absorption ratio per unit integrated absorption of a semi-infinite porous medium for a frequency range $\Omega = 10^{-2}$ to $\Omega = 10^2$ for the rigidly backed layer (solid line) and porous layer with airgap (dash dotted line)

3.7 Porosity

The value of the impedance used so far in this model refers to the characteristic impedance inside the pores of the medium. It is representative of the impedance of the medium for values of the porosity close to 1. For decreasing values of the porosity, it becomes less representative. Therefore the characteristic impedance Z'_c should be used:

$$Z'_c = \frac{Z_c}{h} \quad (3.75)$$

where h is the porosity.

Figure 3.28 shows plots for the real and imaginary parts of the characteristic impedance where the thick line represents Z'_c for $h = 0.4$, and Figure 3.29 represents the real and imaginary parts of the corresponding reflection coefficient. Finally Figure 3.30 shows the absorption coefficient plots for the two cases. The reference semi-infinite plots are given for the two cases of Z_c and Z'_c

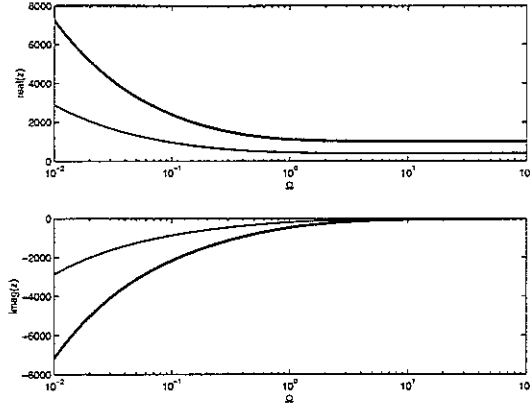


Figure 3.28 Real and imaginary part for the acoustic impedance: Z_c thin line, Z'_c thick line ($h=0.4$)

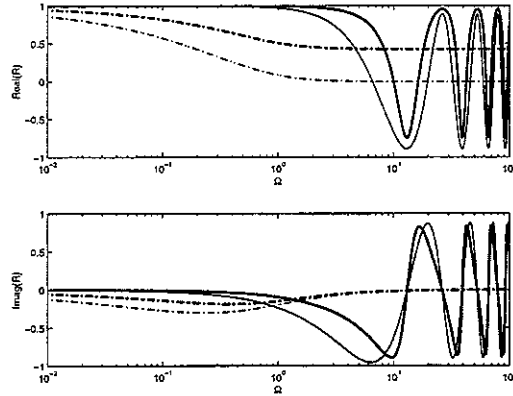


Figure 3.29 Real and imaginary part for the reflection coefficient: R for Z_c thin line, R for Z'_c thick line ($h=0.4$) The dash dotted lines represent the corresponding cases for the semi-infinite medium

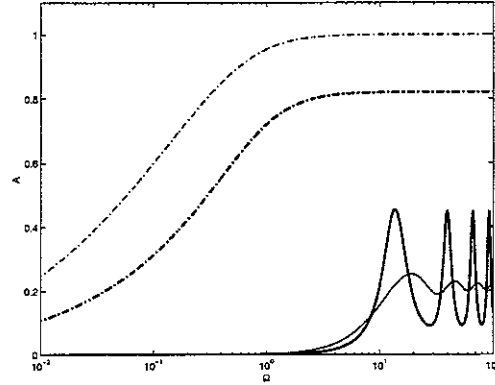


Figure 3.30 Absorption coefficient: A for Z_c thin line, A for Z'_c thick line ($h=0.4$). Corresponding reference semi infinite cases dash dotted lines

The height of the plateau for the semi-infinite case when using Z'_c instead of Z_c (thick dash-dotted line in figure 3.30) is given by:

$$A_{\text{plateau}} = \frac{4h}{(1+h^2)} \quad (3.76)$$

4 CONCLUDING REMARKS

The study presented in this report is concerned with the acoustic properties of rigid frame porous materials. The aim was to investigate the acoustic absorption effects of such kind of materials by using simple formulae based on a macroscopic model of the absorption effects. After an introduction on theoretical foundations of wave propagation, the wave equations inside the material were derived, with reference to a semi-infinite or finite thickness medium. The sound pressure inside and outside the material can, in fact, lead to the definition of reflection and transmission coefficients. Distinction has been made between two kinds of coefficients, i.e. those concerning a single interface between two media, and those concerning a finite thickness layer.

In the case of a layer with rigid backing, reflection coefficients have been compared with established relations and have been used for the computation of absorption coefficients. It can be seen that acoustic absorption for these kinds of materials grows from 0 to a plateau value as the frequency rises.

An extension of the work first concerns the study of sound transmission through a finite thickness layer and then the analysis of the absorption of a layer placed at a certain distance from a rigid wall. Transmission through the layer causes the absorption coefficient to assume higher values in the low frequency region, due to the absence of reflection from a rigid surface. The analysis has also highlighted that the thinner the layer the greater is the absorption coefficient.

For the case with an air gap between the layer and the rigid backing, results show that the behaviour is to some extent similar to the case of rigid backing. Indeed for a fixed cavity depth the height of the plateau is the same for the two cases. In contrast, for a fixed thickness of the layer, the absorption curves for the air gap case show the first peak of absorption at lower frequencies. It is the thickness of the layer that governs the value of absorption at high frequency. The air gap is, instead, responsible for shifts of absorption peaks in the frequency range. A particular case is that of a fixed sum of thickness and cavity depth: while varying simultaneously these two parameters in order to have a constant sum, it can be noticed that the frequency of the main peak is almost constant.

With this work a general formulation based on propagating waves has been derived. Furthermore, sets of plots that characterise the most important absorption features and mechanisms have been clearly highlighted. A set of practical conclusions for the design of absorption treatments are also given which can be summarised with the following points:

1. if the target is to have a good absorption with little space available, one has to bear in mind that the thicker the porous layer, the higher is the absorption at high frequencies;
2. besides this, the frequency at which the peak of absorption occurs does not practically change while keeping constant the sum of layer thickness and cavity depth;
3. the increase of the air gap, given a fixed thickness of the layer, is quite effective in moving the peak of absorption towards lower frequencies as compared to the one of the rigid backing case. Though, if the cavity is deep relative to the thickness of the porous layer d then there may be several frequencies for which the cavity depth is alternately one quarter wave, then one half wave, deep. This can cause the absorption coefficient to vary between low and high values.

APPENDIX A

DERIVATION OF THE ACOUSTIC WAVE EQUATION AND SIMPLE SOLUTION

In order to derive simple equations that describe sound propagation in a fluid a few assumptions are necessary. First the fluid is considered as lossless, so that there are no dissipative effects due to viscosity or heat conduction; for waves of relatively small amplitude, changes in the density of the medium can be considered small compared with the equilibrium state.

The well-known *equation of state* can be simplified if the thermodynamic process is restricted. This is the case of perfect gas isothermal conditions:

$$P / P_0 = \rho / \rho_0 \quad (\text{A.1})$$

where P is the instantaneous pressure at the generic position (x,y,z)

P_0 is the equilibrium pressure at (x,y,z)

ρ is the instantaneous density at (x,y,z)

ρ_0 is the equilibrium density at (x,y,z)

or, assuming adiabatic conditions:

$$P / P_0 = (\rho / \rho_0)^\gamma \quad (\text{A.2})$$

where γ is the ratio of the specific heats.

For fluids other than a perfect gas, the adiabatic case becomes more complicated and it is preferable to determine experimentally the isentropic relationship between pressure and density fluctuations. This relationship can be represented by a Taylor's expansion around $\rho = \rho_0$ (Kinsler *et al.*, 2000):

$$P = P_0 + \left(\frac{\partial P}{\partial \rho} \right)_{\rho_0} (\rho - \rho_0) + \frac{1}{2} \left(\frac{\partial^2 P}{\partial \rho^2} \right)_{\rho_0} (\rho - \rho_0)^2 + \dots \quad (\text{A.3})$$

where the partial derivatives are determined for the isentropic compression and expansion of the fluid about its equilibrium density.

If the fluctuations are small, only the lowest order term in $(\rho - \rho_0)$ need be retained. This gives a linear relationship between the pressure fluctuation and the change in density

$$P = P_0 + \left(\frac{\partial P}{\partial \rho} \right)_{\rho_0} (\rho - \rho_0) \quad P - P_0 = B(\rho - \rho_0) / \rho_0 \quad (\text{A.4})$$

where $B = \rho_0 (\partial P / \partial \rho)_{\rho_0}$ is the *adiabatic modulus*. Then:

$$p = Bq \quad (\text{A.5})$$

where $q = (\rho - \rho_0) / \rho_0$ is the condensation at (x, y, z) and $p = P - P_0$.

The other important relationship between the particle velocity and the instantaneous density is the **equation of continuity**.

Imagine a small rectangular parallelepiped volume element $dV = dx \, dy \, dz$, which is fixed in space and through which elements of the fluid travel. The net rate, with which mass flows into the volume through its surface, must equal the rate with which the mass within the volume increases. The net influx of mass into this spatially fixed volume resulting from flow in the x direction is

$$\left[\rho u_x - \left(\rho u_x + \frac{\partial(\rho u_x)}{\partial x} dx \right) \right] dy dz = - \frac{\partial(\rho u_x)}{\partial x} dV \quad (\text{A.6})$$

where u_x is the velocity component in the x direction.

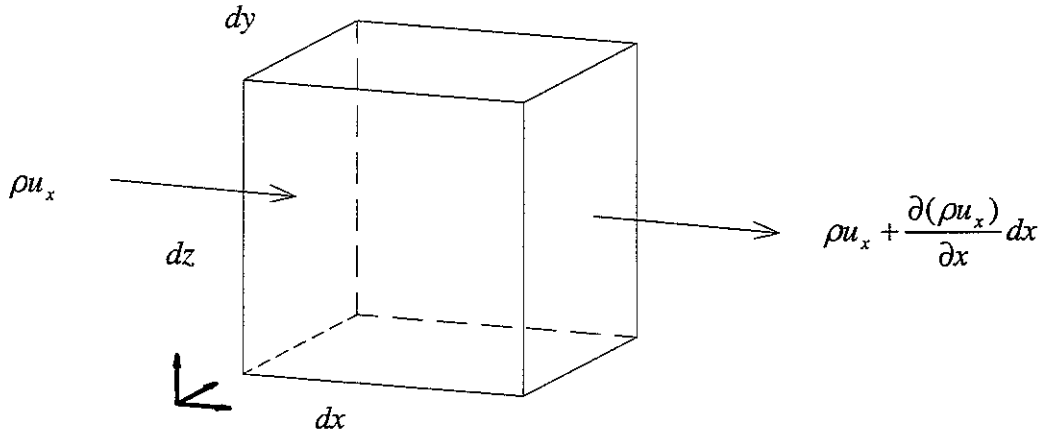


Figure A.1 Flow in the x direction through a parallelepiped volume

By writing similar expressions for the influx in the y and z directions, the total influx can be derived:

$$- \left(\frac{\partial(\rho u_x)}{\partial x} + \frac{\partial(\rho u_y)}{\partial y} + \frac{\partial(\rho u_z)}{\partial z} \right) dV = - \nabla \cdot (\rho \mathbf{u}) dV \quad (\text{A.7})$$

The rate with which the mass increases in the volume is $(\partial\rho/\partial t)dV$. The net influx must equal the rate of increase:

$$\frac{\partial\rho}{\partial t} + \nabla \cdot (\rho\mathbf{u}) = 0 \quad (\text{A.8})$$

Then, if we write $\rho = \rho_0(1+q)$, and assume q is very small gives:

$$\rho_0 \frac{\partial q}{\partial t} + \nabla \cdot (\rho_0\mathbf{u}) = 0 \quad (\text{A.9})$$

The simple force equation: Euler's equation

According to Newton's second law, the net force df_x acting on the same fluid element dV containing a mass dm of fluid, is:

$$df_x = \left[P - \left(P + \frac{\partial P}{\partial x} dx \right) \right] dydz = -\frac{\partial P}{\partial x} dV \quad (\text{A.10})$$

By taking into account the analogous expressions for df_y and df_z , as well as the presence of the gravitational field (with a force $\mathbf{g}\rho dV$), we can write:

$$d\mathbf{f} = -\nabla P dV + \mathbf{g}\rho dV \quad (\text{A.11})$$

In order to obtain an expression for the acceleration, it is possible to start from the Taylor's expansion of the particle velocity, which is a function of both time and space. Thus when the fluid element with velocity $\mathbf{u}(x, y, z, t)$ at position (x, y, z) and time t moves to a new location $(x+dx, y+dy, z+dz)$ at a later time $t+dt$, its new velocity is expressed by:

$$\mathbf{u}(x+u_x dt, y+u_y dt, z+u_z dt, t+dt) = \mathbf{u}(x, y, z, t) + \frac{\partial \mathbf{u}}{\partial x} u_x dt + \frac{\partial \mathbf{u}}{\partial y} u_y dt + \frac{\partial \mathbf{u}}{\partial z} u_z dt + \frac{\partial \mathbf{u}}{\partial t} dt \quad (\text{A.12})$$

Then the acceleration becomes:

$$\mathbf{a} = \lim_{dt \rightarrow 0} \frac{\mathbf{u}(x+u_x dt, y+u_y dt, z+u_z dt, t+dt) - \mathbf{u}(x, y, z, t)}{dt} \quad (\text{A.13})$$

or

$$a = \frac{\partial \mathbf{u}}{\partial t} + u_x \frac{\partial \mathbf{u}}{\partial x} + u_y \frac{\partial \mathbf{u}}{\partial y} + u_z \frac{\partial \mathbf{u}}{\partial z} = \frac{\partial \mathbf{u}}{\partial t} + (\mathbf{u} \cdot \nabla) \mathbf{u} \quad (\text{A.14})$$

Since the mass of the element is ρdV we obtain (from equation A.11):

$$-\nabla P + \mathbf{g}\rho = \rho \left(\frac{\partial \mathbf{u}}{\partial t} + (\mathbf{u} \cdot \nabla) \mathbf{u} \right) \quad (\text{A.15})$$

This is the so called *Euler equation* with gravity. In the case where there is no acoustic excitation, $g\rho_0 = \nabla P_0$, and thus $\nabla P = \nabla p + g\rho_0$ (as $\nabla P - \nabla P_0 = \nabla p$), and so

$$-\frac{1}{\rho_0} \nabla p + \mathbf{g}q = (1+q) \left(\frac{\partial \mathbf{u}}{\partial t} + (\mathbf{u} \cdot \nabla) \mathbf{u} \right) \quad (\text{A.16})$$

If we now make the assumptions that $|gq| \ll |\nabla p|/\rho_0$, $|q| \ll 1$ and that $|(\mathbf{u} \cdot \nabla) \mathbf{u}| \ll |\partial \mathbf{u} / \partial t|$, then $|gq| \ll |\nabla p|/\rho_0$

$$\rho \frac{\partial \mathbf{u}}{\partial t} = -\nabla p \quad (\text{A.17})$$

The linear wave equation

The linearized equations (A.5) (A.8) (A.17) can be combined to obtain a single differential equation with one dependent variable, to give

$$\nabla \cdot \left(\rho \frac{\partial \mathbf{u}}{\partial t} \right) = -\nabla^2 p \quad (\text{A.18})$$

where $\nabla \cdot \nabla = \nabla^2$ is the three dimensional Laplacian operator.

If we take the time derivative of (A.9), and consider space and time as independent and that ρ_0 is only a weak function of time, gives

$$\rho_0 \frac{\partial^2 q}{\partial t^2} + \nabla \cdot \left(\rho_0 \frac{\partial \mathbf{u}}{\partial t} \right) = 0. \quad (\text{A.19})$$

Combining the equations (A.18) and (A.19) gives

$$\nabla^2 p = \rho_0 \frac{\partial^2 q}{\partial t^2} \quad (\text{A.20})$$

As the condensation can be written as $q = p/B$, and as B is a weak function of time, the *linear, lossless wave equation* for the propagation of sound in fluids with phase speed c is:

$$\nabla^2 p = \frac{1}{c^2} \frac{\partial^2 p}{\partial t^2} \quad (\text{A.21})$$

where c is the *thermodynamic speed of sound* defined by

$$c^2 = \frac{B}{\rho_0} \quad (\text{A.22})$$

The above derivation did not require a restriction on B or ρ_0 with respect to space, therefore it is valid for propagation in media with sound speeds that are functions of space, such as found in the atmosphere or the ocean.

APPENDIX B

COMPLEX AND EXPONENTIAL REPRESENTATION OF HARMONIC FUNCTIONS

One of the most useful ways of describing simple harmonic motion is obtained by regarding it as the projection of uniform circular motion onto a perpendicular plane (French, 1971), as shown in Figure B.1.

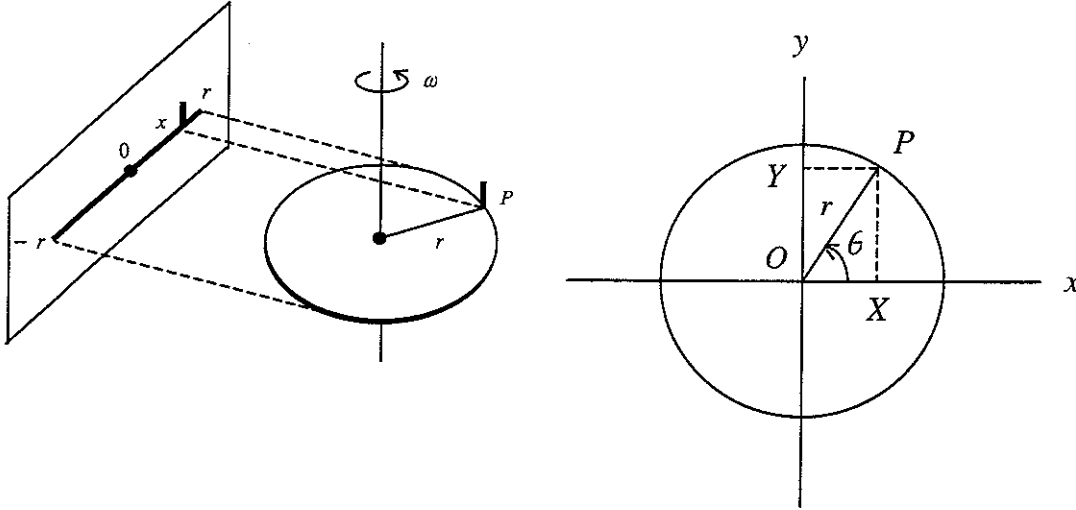


Figure B.1 *Representation of projection of circular motion*

Referring to Figure B.1, the instantaneous position of the point P is then defined by the constant length A and the variable angle θ . By taking the counterclockwise direction as positive, the actual value of θ can be written:

$$\theta = \omega t + \varphi, \quad (\text{B.1})$$

where φ is the value of θ at $t = 0$. Then the displacement of the actual motion is given by:

$$x = r \cos \theta = r \cos(\omega t + \varphi). \quad (\text{B.2})$$

The circular motion defines SHM (simple harmonic motion) of amplitude A and angular frequency ω along any straight line in the plane of the circle. By considering the y -axis perpendicular to the real physical axis, it can be observed that the rotating vector OP defines, in addition to the oscillation along x , an accompanying orthogonal oscillation along y , such that

$$\begin{cases} x = r \cos(\omega t + \varphi) \\ y = r \sin(\omega t + \varphi) \end{cases} \quad (\text{B.3})$$

The rotating vector, with tail anchored in O and tip corresponding to the point P rotating with constant angular speed ω in Figure B.1, has the polar coordinates (r, θ) . The rectangular (Cartesian) components of this vector (x, y) are defined by the equations:

$$\begin{aligned} x &= r \cos \theta \\ y &= r \sin \theta \end{aligned} \quad (\text{B.4})$$

The complete vector \mathbf{r} can then be expressed as the vector sum of these two orthogonal components:

$$\mathbf{r} = x\hat{\mathbf{i}} + y\hat{\mathbf{j}} = r \cos \theta \hat{\mathbf{i}} + r \sin \theta \hat{\mathbf{j}} \quad (\text{B.5})$$

where $\hat{\mathbf{i}}$ and $\hat{\mathbf{j}}$ are the unit vectors in the x and y directions respectively.

However, a convenient form of describing rotating vectors, e.g. phasors, is given by the complex notation. In this case the x -axis represents the real axis and the y -axis the imaginary one, as shown in Figure B.2.

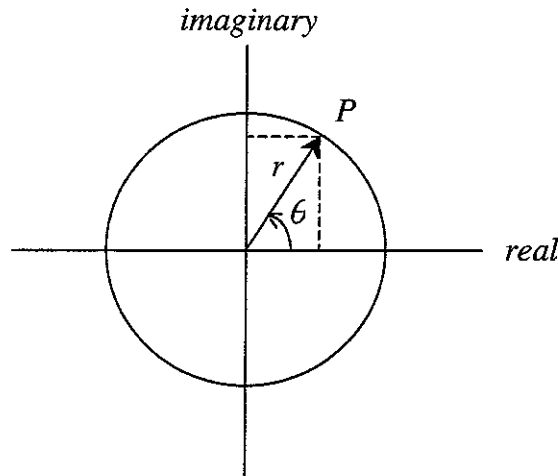


Figure B.2 Gaussian representation of a rotating vector

In this way the vector can be written as

$$\mathbf{r} = x + jy = r \cos \theta + jr \sin \theta \quad (\text{B.6})$$

where x is the real component, y the imaginary one and $j = \sqrt{-1}$

The exponential complex notation can be used, upon which a complex number may be described by the expression:

$$\mathbf{r} = re^{j\theta} = r \cos \theta + jr \sin \theta \quad (\text{B.7})$$

where, as previously $x = r \cos \theta$ and $y = r \sin \theta$ and thus

$$\frac{x}{y} = \tan \theta \quad \text{and} \quad r = \sqrt{x^2 + y^2} \quad (\text{B.8})$$

This notation is widely used as it is far simpler than the previous one (with sine and cosine) in the development of algebraic and analytical operations.

Solution for the simple harmonic motion equation

The relations presented so far can now be used to obtain a solution for the *simple harmonic motion equation*.

The linear differential equation, which represents the motion of a simple oscillator is:

$$\frac{d^2 x}{dt^2} + \omega_0^2 x = 0 \quad (\text{B.9})$$

where ω_0 is the circular frequency of the oscillatory motion

A general approach to solving these equations, is to assume a solution of the form

$$x = Ae^{\zeta t} \quad (\text{B.10})$$

Substitution gives $\zeta^2 = -\omega_0^2$ or $\zeta = \pm j\omega_0$. Thus the general solution is

$$x = A_1 e^{j\omega_0 t} + A_2 e^{-j\omega_0 t} \quad (\text{B.11})$$

where A_1 and A_2 are to be determined by initial conditions $x(0) = x_0$ and $dx(0)/dt = u_0$. This results in two equations:

$$A_1 + A_2 = x_0 \quad \text{and} \quad A_1 - A_2 = \frac{u_0}{j\omega_0} = \frac{-ju_0}{\omega_0} \quad (\text{B.12})$$

from which

$$A_1 = \frac{1}{2} \left(x_0 - \frac{ju_0}{\omega_0} \right) \quad \text{and} \quad A_2 = \frac{1}{2} \left(x_0 + \frac{ju_0}{\omega_0} \right) \quad (\text{B.13})$$

are complex conjugates. Substitution of A_1 and A_2 into equation (B.11) yields:

$$x = x_0 \cos \omega_o t + \frac{u_0}{\omega_o} \sin \omega_o t . \quad (\text{B.14})$$

It can be noticed that satisfying the initial conditions caused the imaginary part of x to vanish. In practice it is unnecessary to go through the mathematical steps required to make the imaginary part of the general solution vanish, for the real part of the complex solution is by itself a *complete general solution* of the original real differential equation.

This means that of a general solution of the form

$$x = Ae^{j\omega_o t} \quad (\text{B.15})$$

where $A = a + jb$, only the real part is considered

$$\text{Re}\{x\} = a \cos \omega_o t - b \sin \omega_o t \quad (\text{B.16})$$

The expression $\exp(j\omega_o t)$ may be thought of as a *phasor* f of unit length rotating counterclockwise in the complex plane with angular speed ω_o . Similarly any complex quantity $A = a + jb$ may be represented by a phasor of length $A = \sqrt{a^2 + b^2}$, making an angle $\phi = \tan^{-1}\left(\frac{b}{a}\right)$ counterclockwise from the positive real axis. Consequently the product $A \exp(j\omega_o t)$ represents a phasor of length A and initial phase angle ϕ rotating in the complex plane with angular speed ω_o . The real part of this rotating phasor (its projection on the real axis) is

$$A \cos(\omega_o t + \phi) \quad (\text{B.17})$$

and varies harmonically with time.

APPENDIX C

DEFINITION OF THE VARIABLE USED IN SECTION 3

In section 3 a few variables have been introduced, which derive from the work in (Brennan and To, 2001). They mainly concern impedance and wavenumber as function of the normalised frequency defined in § 3.3.4. These definitions include some parameters which refer to physical and geometrical properties of porous materials (Johnson *et al.*, 1987, Lafarge *et al.*, 1997).

The definition of wavenumber and impedance is derived from the definition of effective density:

$$\frac{\rho_e}{\rho_0 \alpha_\infty} = \left(1 + \frac{1}{j\Omega} \left(1 + j\Omega \frac{M}{2} \right)^{\frac{1}{2}} \right)$$

where

$M = \frac{8\alpha_\infty k_0}{h\Lambda^2}$ is the non-dimensional shape factor that depends on the microstructure of the material,

α_∞ is the tortuosity

h is the porosity

γ is the ratio of specific heats

$$k_0 = \frac{\omega}{c_0}$$

c_0 is the speed of sound in air

$$\Omega = \frac{\omega}{\omega_t} \quad \text{with} \quad \omega_t = \frac{h\eta}{k_0 \rho_0 \alpha_\infty}.$$

The complex *wavenumber* with M set to zero is defined as

$$k_c = k_0 \left(\frac{\alpha_\infty \gamma}{2\Omega} \right)^{\frac{1}{2}} \left\{ \left((\Omega^2 + 1)^{\frac{1}{2}} + \Omega \right)^{\frac{1}{2}} - j \left((\Omega^2 + 1)^{\frac{1}{2}} - \Omega \right)^{\frac{1}{2}} \right\} \quad (\text{C.1})$$

The complex impedance with M set to zero is defined as:

$$Z_c = Z_0 \left(\frac{\alpha_\infty}{2\gamma\Omega} \right)^{\frac{1}{2}} \left\{ \left((\Omega^2 + 1)^{\frac{1}{2}} + \Omega \right)^{\frac{1}{2}} - j \left((\Omega^2 + 1)^{\frac{1}{2}} - \Omega \right)^{\frac{1}{2}} \right\} \quad (\text{C.2})$$

Specific values for the parameters are those given in table C.1.

Porosity h	0.4
Viscous permeability k_0	1.5 e-9 m^2
Tortuosity	1.37
Density ρ_0 at 20 C	1.2 kg m^{-3}
Dynamic viscosity η at 20 C	$18.22 \text{ e-6 Ns m}^{-2}$
Ratio of specific heats γ	1.4

Table C.1 *Values of the parameters used in the definitions of wavenumber and impedance*

These definitions apply to the general case of a semi-infinite medium and they have been used in the present work.

In the case of a layer with rigid backing, the normal incidence impedance is defined as follows:

$$Z_f = j \frac{Z_c}{h} \cot(k_c d). \quad (\text{C.3})$$

This equation has not been used in the present study to calculate absorption coefficients, as they have been derived from calculated reflection coefficient for the case of a porous material with rigid backing. However results obtained have been compared with those gained with this formula and have proved to be equal.

REFERENCES

- Allard, J. F. (1993). *Propagation of sound in porous media*, London, Elsevier Applied Science
- Bies, D. A, and Hansen, C. H. (1980). "Flow Resistance information for acoustical design", *Applied Acoustics* **13**, 357-391
- Brennan, M. J., and To, W. M. (2001). "Acoustic properties of rigid frame porous materials – an engineering perspective", *Applied Acoustics* **62** 793-811
- Fahy, F. (2001). *Foundations of Engineering Acoustics*, (Academic Press)
- French, A. P. (1971). *Vibrations and Waves* (Stanley Thornes Publishers Ltd)
- Johnson, D. L., Koplik, J., and Dashen, R. (1987). "Theory of dynamic compressibility and tortuosity in fluid-saturated porous media", *J. Fluid. Mech.* **176**, 379-402
- Kinsler, L. E., Frey, A. R., Coppens, A. B., and Sanders, J. V. (2000). *Fundamentals of Acoustics*, Fourth Edition, (John Wiley and Sons, Inc.)
- Kuttruff, H. (1973). *Room Acoustics* (Applied Science Publisher LTD, London)
- Lafarge, D., Lemarinier, P., and Allard, J. F. (1997). "Dynamic compressibility of air in porous structures at audible frequencies", *J. Acoust. Soc. Am.* **102**, 1995-2006
- Richardson, E. G. (1953). *Technical Aspects of Sound* (Elsevier Publishing Company)
- Umnova O., Attenborough K., Li K. M. (2000), "Cell model calculation of dynamic drag parameters in packings of spheres", *J. Acoust. Soc. Am.* **107**, 3113-3119
- Zwikker, C., and Kosten, C. W (1949). *Sound Absorbing Materials* (Elsevier, Amsterdam)